LA-7113-MS
Informal Report

Tunable Lasers for Waste Management Photochemistry Applications

University of California
LOS ALAMOS SCIENTIFIC LABORATORY
Post Office Box 1663 Los Alamos, New Mexico 87545

LA-7113-MS
Informal Report
UC-~~84~~ 70
Issued: September 1978

Tunable Lasers for Waste Management Photochemistry Applications

Compiled by

F. T. Finch

CONTENTS

ABSTRACT 1

I. INTRODUCTION 1

II. CHARACTERISTICS OF DYE LASERS 2
General 2
Dye Characteristics 3
Optical Pumping Methods 11
Optical Cavity Design 12
Dye Laser Efficiency - Wavelength Relationships 16
References 18

III. CHARACTERISTICS OF EXCIMER LASERS 24
General 24
Relevant Molecular Physics 25
Laser Action on Excimer Transitions 30
Electron-Beam-Excited Excimer Lasers 35
Electric-Discharge-Excited Excimer Lasers 40
References 44

IV. CHARACTERISTICS OF TUNABLE IR LASERS 46
Semiconductor Diode Lasers 46
Spin-Flip Raman Lasers 47
Optical Parametric Oscillators 49
Other Nonlinear Techniques 50
Gas Lasers 50
References 51

V. LASER SYSTEM RELIABILITY 51
Welding Lasers 51
Pulsed High-Power CO_2 Lasers 52
Nitrogen Lasers 52
Dye Lasers 52
Solid-State Lasers 53

VI. LASER-SYSTEM SAFETY 53

VII. PROJECTED LASER COSTS 53
Capital Costs 53
Operating Costs 55
References 56

TUNABLE LASERS FOR WASTE MANAGEMENT PHOTOCHEMISTRY APPLICATIONS

Compiled by

F. T. Finch

ABSTRACT

A review of lasers with potential photochemical applications in waste management indicates that dye lasers, as a class, can provide tunable laser output through the visible and near-uv regions of the spectrum of most interest to photochemistry. Many variables can affect the performance of a specific dye laser, and the interactions of these variables, at the current state of the art, are complex. The recent literature on dye-laser characteristics has been reviewed and summarized, with emphasis on those parameters that most likely will affect the scaling of dye lasers in photochemical applications. Current costs are reviewed and correlated with output power.

A new class of efficient uv lasers that appear to be scalable in both energy output and pulse rate, based on rare-gas halide excimers and similar molecules, is certain to find major applications in photochemistry. Because the most important developments are too recent to be adequately described in the literature or are the likely outcome of current experiments, the basic physics underlying the class of excimer lasers is described. Specific cost data are unavailable, but these new gas lasers should reflect costs similar to those of existing gas lasers, in particular, the pulsed CO_2 lasers.

To complete the survey of tunable-laser characteristics, the technical characteristics of the various classes of lasers in the ir are summarized. Important developments in ir laser technology are being accelerated by isotope-separation research, but, initially at least, this portion of the spectrum is least likely to receive emphasis in waste-management-oriented photochemistry.

I. INTRODUCTION

Tunable lasers of one type or another are available which operate from the near-ultraviolet, the visible, the near-infrared, and through the middle-infrared portions of the spectrum. Research is under way to extend the range on both sides of the spectrum, deeper into the infrared (ir) and ultraviolet (uv).

The definition of tunable lasers has been somewhat arbitrary. At one extreme, fine tuning of the cavity of a normal gas laser over the Doppler-broadened width of a reflected line may achieve continuous tuning over a very restricted range ($\sim 0.003\ cm^{-1}$). However, few applications exist for such restricted tuning ranges, and the inclusion of such lasers in our assessment of tunable-laser performance and costs would have been an unmanageable task.

Tunable lasers are usually defined as lasers tunable over a range of 50 to 100 cm^{-1} or more. The tuning may not be continuous over the entire range.

The literature on tunable lasers mostly refers to lasers with very high resolution for applications in spectroscopy, which are not necessarily suited for photochemistry or isotope separations. In this evaluation of tunable lasers for photochemical applications in waste management, emphasis is placed on lasers with output wavelengths in the uv and visible, where most photochemistry occurs, rather than on those in the near- and middle-infrared. Also emphasized are types of lasers that may be scalable to industrial-size devices, particularly dye and excimer lasers. Dye lasers constitute the most versatile class in the spectrum of interest, providing coverage from the uv to the near-ir with further extension into the ir using optical parametric oscillators (OPO) and into the uv with frequency-doubling. Excimer lasers represent a new class of lasers with relatively narrow tuning ranges for any single laser, but with potentially broad coverage of the uv region as a class. There are growing indications that the KrF excimer (or, more precisely, exciplex) laser may come to occupy a role in the uv region analogous to that of the CO_2 laser in the ir.

The tuning ranges for most of the important types of tunable lasers are indicated in Fig. 1. While this figure essentially covers the complete spectrum, it does not contain information on the characteristics of laser light at the various wavelengths. These characteristics, which include laser energy, line width, pulse width, beam quality, efficiency, and others, vary considerably over the spectrum.

II. CHARACTERISTICS OF DYE LASERS

General

Dye lasers are the most versatile class of lasers for laser photochemistry applications. They are available for wavelengths from the near-ir to the uv

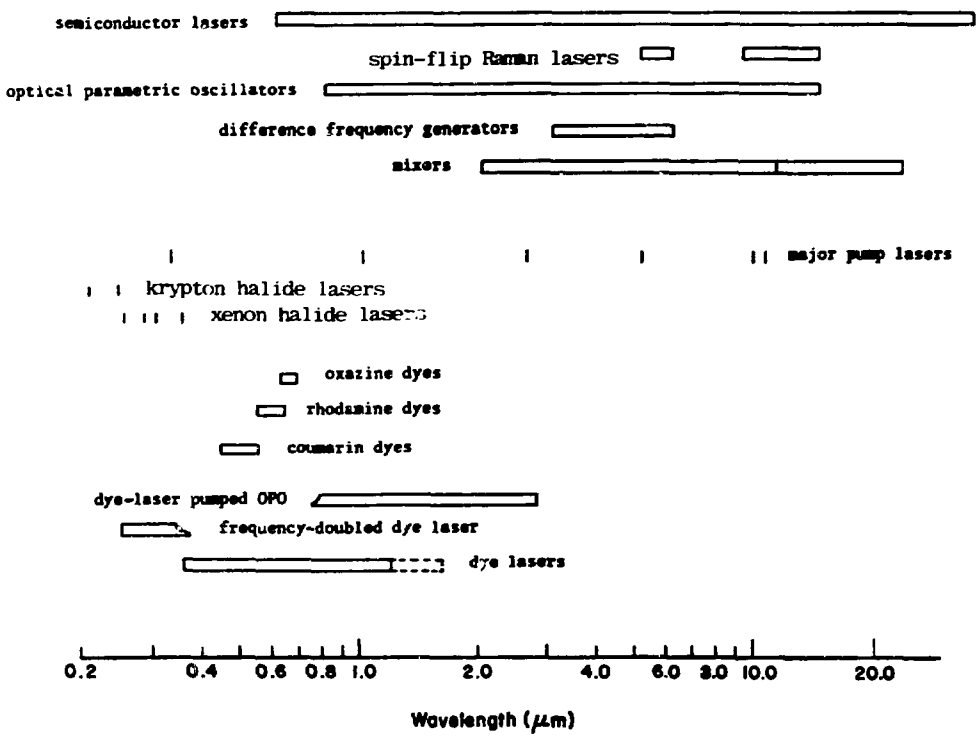

Fig. 1. Ranges of tunable lasers.

(Fig. 1). They can be continuous wave (CW), modelocked to give picosecond pulse chains, or pulsed at intermediate rates. They can be of simple design with fair beam quality or tailored to give specific beam characteristics by more complex design. Liquid-dye lasers are optically pumped, usually by flashlamps or by other lasers. Vapor-phase dye lasers could be pumped electrically. A desired wavelength may be obtained by selecting the proper dye solvent, temperature, optical cavity design, or a combination of these possibilities. The physical configuration of dye lasers may vary widely, depending on the quality of the output. Many variables are involved in the chemical composition of the dye solution and in optical construction of the laser. The interaction of so many variables makes an analysis of dye-laser performance difficult.

Dye-laser characteristics are surveyed in this report. The literature has been reviewed, representatively but not necessarily exhaustively, from 1973 to present, with some significant earlier references included. Characteristics of lasers useful in systems analysis and for a projection of future dye-laser capabilities are stressed. No attempt is made to assemble a compendium of laser dyes. Extensive listings are available elsewhere.[1-6] and new laser dyes are being developed almost daily. Several reviews on dye lasers have been published.[6-11] but none had been prepared specifically to serve as a reference base for systems studies of photochemical applications. Original publications have been used as far as possible. Some patents and foreign-language articles are referenced through Chemical Abstracts.

The versatility of dye lasers derives from the diversity of organic compounds available as laser dyes and the complexity of their interactions with solvents and with each other. The photophysics and photochemistry of laser dyes will be discussed first. Pumping sources and their

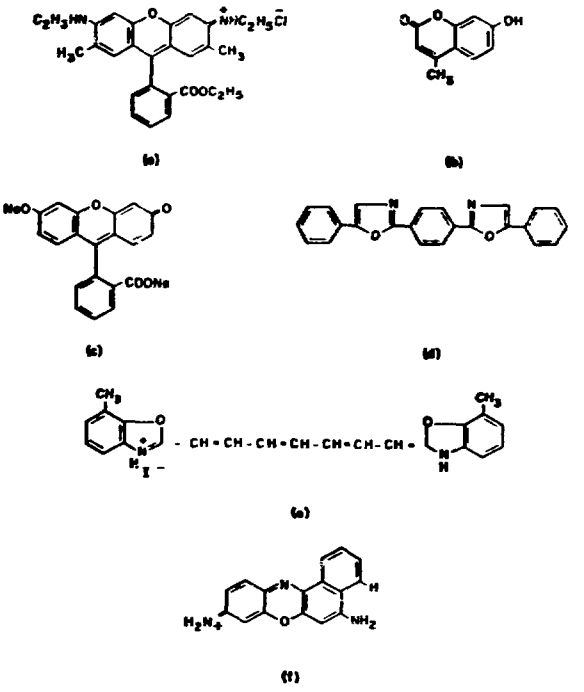

Fig. 2. Typical laser dyes: (a) rhodamine 6G, (b) 4-methylumbelliferone, (c) disodium fluorescein, (d) 1,4-di 2-(5-phenyloxazolyl) benzene (POPOP), (e) 3,3'-dimethyl-2,2'-oxatricarbocyanine iodide (DOTC), (f) cresyl violet.

effects on laser output will then be described, followed by discussion of optical cavity design and tuning mechanisms. The interaction of these design and operating options provides the versatility and potential of dye lasers.

Dye Characteristics

The lasing dye is a complex organic compound, often having twenty or more atoms per molecule and usually displaying a high degree of unsaturation (π-bonding). Figure 2 shows structures of several typical laser dyes. Many compounds used originally in solution lasers were of the class conventionally called dyes. However, many properties of conventional dyes, such as affinity for fibers, are not relevant to laser dyes. On the other hand, many laser dyes do not absorb in the visible part of the spectrum and are therefore colorless to human vision. The common characteristic of laser dyes and conventional dyes is a

molecules at the pumping energy,
subsequent lessened absorption
ing.[32-35] However, the term photobleaching is also used to indicate a more permanent change in the dye solution that apparently results from photochemical reaction. Both effects may interact with, and be difficult to distinguish from, triplet-triplet absorption. Because each dye has its own characteristic energy spacings and reactivity, these effects will contribute differently for each dye.

TABLE I

PERFORMANCE OF DYES LASING AT VARIOUS WAVELENGTHS

Dye	Solvent	Molarity	Pumping Source	Source[a] Energy (J)	Pumping Threshold (J)	λ_{max} Output (nm)	Tuning Range (nm)	Output at λ_{max}	Ref.
p-terphenyl	cyclohexane	9×10^{-3}	xenon plasma	5.6[b]	---	340	---	0.010 J	21
PBD[c]	toluene	5×10^{-3}	nitrogen laser	0.0018	---	---	357-376	~ 20% eff.	2
POPOP[d]	vapor phase	2×10^{-4}	nitrogen laser	0.004	5×10^{-4}	393	---	3×10^{-4} J	22
	dioxane	2×10^{-3}	flashlamp	1.5	0.073	420	---	---	23
	toluene	5×10^{-4}	Nd:YAG laser 3rd harmonic	0.0005	---	---	415-430	1×10^{-3} mJ	24
7-amino-4-methylcoumarin	methanol	5×10^{-4}	flashlamp	1500	---	435	---	2 J	25
	ethanol	---	flashlamp	---	12	436	---	---	26
7-diethylamino-4-methyl-coumarin	ethanol	7.5×10^{-4}	flashlamp	5	---	460	---	2.7 kW	27
	ethanol	2×10^{-4}	Nd:YAG laser 3rd harmonic	0.025	---	---	440-490	0.35 kW	24
4-methylumbelliferone	ethanol w/ 1 N $HClO_4$	5×10^{-3}	nitrogen laser	600	---	500	460-550	50 J	28
rhodamine B	methanol	1.4×10^{-4}	Nd:YAG laser 2nd harmonic	0.240	---	592	586-598	118 mJ	29
cresyl violet perchlorate	methanol	2.5×10^{-4}	Nd:YAG laser 2nd harmonic	0.240	---	647	642-652	102 mJ	29
DOTC[e]	DMSO[f]	2×10^{-4}	flashlamp 60 mm long	---	7.35	815	810-817	6×10^{-4} eff.	30
			110 mm long	---	17	---	825-837	1.5×10^{-4} eff.	30
DTTC[g]	DMSO	2×10^{-4}	flashlamp 60 mm long	---	10.8	885	883-887	10^{-6} eff.	30
			110 mm long	---	17	---	883-887	2×10^{-6} eff.	30
5,5'-dichloro-11-diphenylamino-3,3'-diethyl-10,12-ethylenetri-carbocyanine perchlorate	DMSO	1×10^{-4}	flashlamp	128	---	950	---	0.053 J	4
1,1'-diethyl-1,3-acetoxy-2,2'-quinotetracarbocyanine iodide	DMSO	1.4×10^{-3}	Q-switched ruby laser	0.625	---	1070-1120	1020-1140	1.5 MW	31

[a] For laser sources, laser output is listed; for flashlamps, electrical input is listed.
[b] CO_2 laser pulse energy to produce plasma.
[c] 2-phenyl 5-(4-biphenylyl)-1,3,4-oxadiazole
[d] 1,4-di(2-(5-phenyloxazolyl))benzene
[e] 3,3' diethyl-2,2'-oxatricarbocyanine iodide
[f] dimethylsulfoxide
[g] 3,3' diethyl-2,2'-thiatricarbocyanine iodide

TABLE II

SOLVENT EFFECTS ON PUMPING THRESHOLD

Compound	Solvent	Pumping Source	Threshold
rhodamine B[a]	methanol	---	1.00[b]
	1:3 mixture of $CF_3CH(OH)CF_3$ and water	---	0.72
3-amino-N-methyl-phthalimide[c]	water	ruby laser	1.35
	acetic acid	(second harmonic)	1.76
	isobutane		1.1
	ethanol		1.0
	isopropanol		1.0
	cyclohexanol		1.6
	acetonitrile		1.28
	dimethylformamide		12.
4-amino-N-methyl-phthalimide[c]	glycerine	ruby laser	1.0
	ethanol	(second harmonic)	0.72
	isobutanol		0.61
	isopropanol		0.55
	cyclohexanol		0.52
	dimethylformamide		0.47
	acetonitrile		0.44
	ethyl acetate		0.92
	acetone		1.50
	dioxane		0.55
rhodamine 6G[d]	ethanol	flashlamp	1.00
	methanol		0.77

[a] Ref. 61.

[b] For each compound, the threshold is given in relative units.

[c] Ref. 62.

[d] Ref. 63.

on lasing properties. The interaction of the functional groups with the parent molecule has been studied in some detail.[55,56] These systematic studies suggest that improved laser dyes can be synthesized. Other correlations between molecular structure and dye performance have been investigated.[2,57,58] The large number of atoms in a dye molecule precludes calculation of its properties by quantum-mechanical methods.

Solvents can interact with dye molecules in several ways that affect laser action. Electronic interactions between solvent and dye molecules affect the spacing of energy levels in the dye molecule, and therefore the transitions between energy levels. The solvent can provide or inhibit relaxation or loss mechanisms that interfere with laser action. There may be a reorientation of solvent molecules about the dye molecule as the dipole moment changes for the ground and excited states.[44] In addition, the solvent provides a medium in which chemical changes can take place, and it may influence such chemical changes. Acid-base, monomer-dimer, and isomerization equilibria have been observed for laser dyes. These microscopic changes result in macroscopic changes in laser properties. Dye-tuning ranges depend upon the solvent.[59] *The solvent also affects the polarization* of the emitted light.[60] Solvent effects on threshold pumping energies and wavelengths are given in Tables II[61-63] and III.[64-66] Threshold pumping energy is the minimum input energy required to produce lasing.

Although the most common type of dye laser uses a liquid solution of the dye in $\sim 10^{-3}$ to 10^{-5} molar concentration, both solid and vapor dye lasers have been

TABLE III

SOLVENT EFFECTS ON LASER WAVELENGTHS

Compound	Solvent	Molarity	Pumping Source	λ_{max} Absorption (nm)	λ_{max} Output (nm)	Tuning Range (nm)	Ref.
9-hydroxy-1-methyl-3H-naphtho[2, 1-b]pyran-1-one	basic	---	nitrogen	420	635	616-686	64
	ethanol	---	laser	346	460	---	64
	conc acid	---		388	550	539-581	64
9-hydroxy-1-trifluoromethyl-3H-naphtho[2,1-b]pyran-3-one	basic	---		530	610	---	64
	ethanol	---		365	520	---	64
	conc acid	---		415	600	---	64
8-hydroxy-4-methyl-2H-naphtho[1, 2-b]pyran-1-one	basic	---		402	530	520-573	64
	ethanol	---		358	430	---	64
	conc acid	---		382	480	484-529	64
8-hydroxy-4-trifluoromethyl-2H-napthо[1,2-b]pyran-2-one	basic	---		440	635	---	64
	ethanol	---		380	485	485-560	64
	conc acid	---		398	530	---	64
8-hydroxy-4-phenyl-2H-naphtho[1, 2-b]pyran-2-one	basic	---		420	610	---	64
	ethanol	---		365	470	---	64
	conc acid	---		333	480	to 490	64
4-methylumbelliferone	ethanol	1×10^{-2}	nitrogen	---	400	---	65
	+ 3% water		laser	---	---	406-435	65
	+ 4% water			---	---	402-535	65
	+ 6% water			---	---	415-558	65
	+ 9% water			---	---	406-52[illegible]	65
	+ 20% water			---	---	425-505	65
	+ HCl		ruby laser	325	490&525	480-540	66
	+ 10% water		2nd harmonic	325	445&482	443-490	66
	+ 40% water			325	470	450-481	66
	ethanol + 0.1/0.24[a]	1×10^{-2}	ruby laser 2nd harmonic	---	525	520-530	66
	+ 0.5/1.0			---	490	480-500	66
	+ 1.0/2.4			---	490	480-500	66
	+ 1.5/3.6			---	485	475-4[illegible]	66
	+ 2.0/4.7			---	480	470-[illegible]	66
	+ 3.0/7.1			---	450	443-470	66
4-amino-N-methylphthalimide	water	---	ruby laser	---	519	---	63
	glycerine	---	2nd harmonic	---	512	---	63
	acetic acid	---		---	512	---	63
	isobutane	---		---	498	---	63
	ethanol	---		---	500	---	63
	isopropanol	---		---	498	---	63
	cyclohexanol	---		---	501	---	63
	acetonitrile	---		---	498	---	63
	dimethylformamide			---	500	---	63
4-amino-N-methylphthalimide	glycerine	---	ruby laser	---	576	---	63
	ethanol	---	2nd harmonic	---	539	---	63
	isobutanol	---		---	536	---	63
	isopropanol	---		---	533	---	63
	cyclohexanol	---		---	528	---	63
	dimethylformamide			---	509	---	63
	acetonitrile	---		---	509	---	63
	ethyl acetate			---	480	---	63
	acetone	---		---	480	---	63
	dioxane	---		---	475	---	63
rhodamine B	methanol	1.4×10^{-4}	Nd:YAG doubled	---	592	486-598	29
	ethylene glycol	2×10^{-4}		---	605	599-611	29
cresyl violet perchlorate	methanol	2.5×10^{-4}	Nd:YAG doubled	---	647	642-652	29
	DMSO	2.5×10^{-4}		---	665	658-672	29
1,1'-diethyl-4,4'-quinotricarbocyanine iodide	acetone	1×10^{-3}	ruby laser	---	1000-1100	970-1125	31
	DMSO	2.5×10^{-3}		---	1050-1110	1020-1140	31

a - First number is molarity of $HClO_4$; second number is molarity of water.

operated. In the solid lasers, a dye-doped polymer has been the lasing medium.[67-69] Solid-dye lasers have found limited application because of heating damage to the matrix and rapid degradation of the dye. The dye 1,4-di[2-(5-phenyloxasyl)]benzene (POPOP) was the first to be made to lase in the vapor phase;[22,70-72] p-terphenyl has also been reported to lase in the vapor phase.[73] With dyes that vaporize without decomposition particle densities comparable to those in solution can be obtained, giving comparable power output. The output of vapor-phase dye lasers can be tuned in the same manner as that of solution lasers. Their output wavelength is shifted toward the blue relative to the solution lasers. A potential advantage of vapor-phase dye lasers is the use of electrical pumping, leading to higher efficiencies in converting input energy to laser output. Electrical pumping has been proposed for solution dye lasers,[74,75] but there are no reports of its success, and decomposition of both dye and solvent appears to pose a formidable obstacle. Conditions required for lasing in the vapor phase may be more stringent than those for the liquid phase.[76,77] Gas-phase dye lasers are reviewed in Ref. 78.

Equations for determining solvent effects on energy spacing have been developed.[60] However, many needed molecular parameters are not available either for the laser dyes or for the solvents. A maximum energy difference between excited and ground states implies a minimum threshold pumping energy. A change from protonated solvents to deuterated solvents has marked effects on lasing properties,[5] probably because of changes in energy-transfer rates. Changes in solvent are known to affect fluorescence yields.[59,79] Triplet population can also be changed.[79] Viscosity of the solvent apparently affects the populations of the various states.[35]

For cw lasers, solvent requirements are more stringent than for pulsed dye lasers.[79] In addition to dissolving the dye, being chemically stable and easy to handle (reasonable vapor pressure and low toxicity), the solvent must be able to dissipate the heat resulting from the high pumping power densities required and must have good viscosity properties for rapid flow (10 cp or higher at room temperature). For example, a mixture of ethanol and water gives better results with rhodamine 6G than ethanol alone, presumably because of the higher specific heat of the water.[80]

The concentration of a dye in solution affects laser characteristics. Lifetimes of the various states are related to concentration, and self-absorption of the emitted light may take place. Concentration effects have been studied both theoretically and experimentally for rhodamine-B[81] and rhodamine-6G.[81,82] Values for the variation of pumping threshold with concentration are given in Table IV.[81-83] Typically, the pumping threshold is high at very low concentrations, decreases to a minimum, then increases again at the highest concentrations. The optimum concentration differs for different dyes and different cavity configurations. The wavelength of laser output is also affected by dye concentration in solution. The amount depends on the dye. The wavelength shift for rhodamine-6G is 30 nm for a change in molarity from 8×10^{-8} to 2×10^{-6} M, whereas it is only 2 to 3 nm for pthalimide derivatives.[84]

Chemical equilibria can play an important part in dye-laser performance. Dye molecules contain functional groups that may participate in acid-base equilibria, such as NH_2, -OH, and -COCH. In addition, the excited states of the molecules may have different acidity properties from the ground state and form complexes (excimers) that do not exist in the ground state. The dye 4-methylumbelliferone lases from several species in solution, giving a tuning range of 176 nm. Complete details of the species involved in the fluorescence and the mechanisms of their formation have not been determined.[63,64,85-91]

TABLE IV

CONCENTRATION DEPENDENCE OF PUMPING THRESHOLD

Dye	Solvent	Concentration (M)	Pumping Threshold	Pumping Source	Ref.
perylene	benzene	3×10^{-3}	22.5 keV	nitrogen laser	83
		6×10^{-3}	19.5 keV		
rhodamine B	water	5×10^{-6}	42[a]	doubled YAG laser	81
		5×10^{-5}	8[a]		
		5×10^{-4}	4[a]		
		5×10^{-3}	71[a]		
	methanol	5×10^{-6}	25[a]		
		5×10^{-5}	7[a]		
		5×10^{-4}	3[a]		
		5×10^{-3}	12[a]		
		5×10^{-2}	124[a]		
rhodamine 6G	water	5×10^{-6}	27[a]		
		5×10^{-5}	27[a]		
		5×10^{-4}	4[a]		
		5×10^{-3}	58[a]		
	methanol	5×10^{-6}	10[a]		
		5×10^{-5}	1[a]		
		5×10^{-4}	1[a]		
		5×10^{-3}	8[a]		
		5×10^{-2}	70[a]		

[a] Normalized to 1 for rhodamine 6G in methanol at 2.5×10^{-4} M.

Dye molecules may associate to form dimers or high clusters. Monomer-dimer equilibria are believed to be important for lasing action in rhodamines,[92,93] but these effects have also been attributed to acid-base equilibria.[94-96] Lasing emission from 7-alkylaminocoumarins has been attributed to a dimer exciplex.[96] The observed improvement of lasing action by the addition of surfactants[92,97] has been attributed to the breaking up of dimers by the formation of micelles containing the individual dye molecules,[92] but micellar formation will affect triplet properties and acid-base equilibria as well. Mixed aqueous-organic solvents are found to give improved laser action with rhodamine-6G because of water's thermal properties combined with the organics' solvation properties.[93] Superradiant emission bands have been observed in concentrated aqueous solutions of rhodamine-B and rhodamine-6G that are attributed to the dimer; addition of a surfactant quenches these bands.[98]

Another reaction that may occur is isomerization; its equilibrium is affected by the solvent.[18] If laser emission occurs from one isomer but not another, solvents favoring the lasing isomer will give better performance.

Temperature effects in dye lasers are related to solvation. Polymethine dyes have been studied in several solvents at temperatures as low as 4.2 K.[99] Generally, lowering the temperature leads to emission at shorter wavelengths and a lower pumping threshold. In some solvents, the quantum yield of fluorescence may increase Below temperatures at which the solvent viscosity reaches 10^{11} P, the lasing spectrum becomes a series of lines.

Sensitization, or energy transfer, a technique used in organic photochemistry,[100] can also be applied to dye lasers. If a light source for the absorption band of the compound of interest is unavailable, a sensitizer can be used to absorb the available light and transfer the energy to the compound of interest. The transfer may result from fluorescence of the sensitizer in the absorption band of the compound of interest (radiative transfer), from collisional transfer, or from long-range electric dipole or quadrupole interaction. Sensitizers may be used either to enhance absorption with a laser source having a wavelength that is poorly absorbed by the dye from which laser action is desired, or to improve the operation of a flashlamp pumped laser. Laser dyes themselves are excellent sensitizers for other laser dyes.

Radiative transfer can take place if the sensitizer and lasing dyes are in separate containers or if they are mixed in the same solution. Dye sensitizer solutions have been circulated between flashlamp pump and the laser dye.[67,101,102] Two dye lasers can be inserted in a single optical cavity, with independent tunability of both beams.[103] Because not all dyes have the same optimum solvent, a double-compartment dye cell is useful.[90] The efficiency of energy transfer may be improved when the sensitizer and the dye are present in the same solution.[83,104] In a dye mixture with multiple-wavelength operation, radiative transfer is the dominant energy-transfer mechanism.[105] To give a particular case, cresyl violet is a poor laser dye unless it is pumped by rhodamine-6G.[6,106,107] The pumping thresholds of other dyes have been reduced by the addition of a sensitizer.[83]

Degradation of laser dyes is a potential problem that will affect the operation of industrial-scale lasers in photochemical applications. The literature is somewhat inconsistent on this issue, and contains ambiguous terminology and unclear distinctions between transient and permanent effects.[108] Hole-burning is a transient effect that results in limited absorption of the pumping radiation and lessened efficiencies. "Photobleaching" has been used to refer to this effect and to another phenomenon that apparently results from photochemical and thermal reactions of the dye to produce nonlasing species or species that absorb at the laser wavelength. Of these two effects, photochemical decomposition may be more serious with regard to the economics of laser operation. With photochemical decomposition, the absorption spectrum of the laser dye changes negligibly, indicating that only small amounts of the degradation products are present in the solution. However, small quantities of impurities are known to have large effects on laser performance.[109] Decomposition products are likely to be fairly similar to the dye in molecular structure, resulting in high energy-transfer rates and quenching the excited states of the dyes. Small changes in structure can also change the light absorption properties significantly, leading to absorption at the laser wavelength.[110] Rates of dye degradation have been studied,[111,112] and the triplet state has been suggested as an important pathway for dye degradation.[113,114] Additional studies of the degradation products and the probable mechanisms of their formation are needed to produce information on designing dye molecules to resist degradation. Some dyes are known to degrade differently from pulsed flashlamp irradiation and irradiation by a mercury line.[115] The photochemical degradation products of one dye, 7-diethylamino-4-methylcoumarin, have been isolated and identified.[110]

The effects of dye degradation can be minimized in several ways. Large quantities of solution circulated through the laser provide for dilution of the degradation products and their possible regeneration, if the reaction is reversible. Addition of surfactants increases the stability of some dyes.[97] The most effective way to eliminate

degradation may be to develop less reactive dyes.[27,110,115,116] A solution of a fluorinated coumarin in dioxane, circulated through a dye cell pumped by a 5-J flashlamp and cooled, has produced 3×10^5 pulses from 500 ml before the pulse power declined to half the original power.[27] The corresponding unfluorinated coumarin produced 1% as many pulses before the pulse power declined by half.

Optical Pumping Methods

Flashlamps or other lasers are generally used to pump liquid dye lasers. Flashlamp pumping is suitable only for pulsed lasers; cw lasers require laser pumping, usually with an argon-ion laser. Flashlamps must produce a pulse of light with a risetime on the order of nanoseconds to pump dyes efficiently. While many dyes can be pumped with flashes having slower risetimes, the energy-conversion efficiency is less than optimum. Although flashlamps have several disadvantages relative to lasers as pumping sources, they are simple, efficient devices producing high optical fluxes.

A coaxial geometry in which a flashlamp is an annulus around the dye channel is favored,[6,117,118] although linear and spiral flashlamps are also used. Ideally, the dye is illuminated uniformly by the flashlamp, requiring a uniform discharge throughout a coaxial flashlamp, but this is seldom achieved. A number of gases can be used for filling the flashlamp. Xenon is common, but krypton, argon, and air are also used. The gas pressure in the flashlamp must be high enough to prevent premature breakdown, but flash intensity varies little with gas pressure.[119] Increasing pressure increases the flash risetime.[23] The fast risetimes required are achieved by using low-inductance capacitors with short connections to the flashlamp. Pyrex is a suitable material for the flashlamp and dye cell if the laser is to be pumped with visible light,[119,120] but quartz is necessary for uv pumping.

Flashlamps have been designed with epoxy-resin seals, or as all-glass or all-quartz systems. The all-quartz systems give the longest lifetimes.[118] A rapid repetition rate can be obtained by thyristors. Flashlamp life is prolonged by operating the flashlamp with a continuous simmering current and triggering by thyristors rather than spark gaps.[101] Large coaxial flashlamp-pumped dye lasers have been built. Outputs of 100 and 400 J have been reported, using rhodamine-6G.[121,122]

The efficiency of a flashlamp-pumped dye laser depends on the flashlamp driver circuit, the characteristics of the optical cavity, the characteristics of the dye, its concentration in solution, and the dye-cell size. Dynamic mathematical models have been formulated to evaluate the effects of these parameters.[36,38,82,117] Efficiencies for conversion of electrical energy are on the order of 1%.[25,117] Rhodamine-6G performance with pumping by flashlamp and by a xenon plasma is given in Table V.[122-124]

Some dyes require a high energy density for pumping, and high energy densities can lower pumping thresholds.[124] A small-diameter dye cell with a coaxial flashlamp is useful in these cases.

Shortcomings of flashlamp-pumped dye lasers are the propagation of inhomogeneities caused by heating through a dye solution and the formation of shock waves from the discharge.[92,117,123,125-128] Inhomogeneities can also result from turbulence associated with a fast flow rate.[129] Inhomogeneities shorten the pulse and distort beam quality, particularly in the dispersive cavity required for tuning.[61] Repetition rates may be limited by the time required for the inhomogeneities to disappear.[5] Using a transverse laser cavity is one approach to minimizing this effort. An elaborate solution to the problem is to flow the dye solution through a zigzag channel in an array of prisms, with two linear flashlamps outside the array.[123] A simpler solution is to introduce an annulus

TABLE V

RHODAMINE-6G LASER CHARACTERISTICS WITH INCOHERENT PUMPING

Rise Time (ns)	Flash Duration (FWHM) (ns)	Input Energy[a] (J)	Output Wavelength (nm)	Pumping Threshold (J)	Output Energy (J)	Efficiency (%)	Solvent	Molarity	Ref.
2800	4000	---	---	15.3	---	---	ethanol	5×10^{-5}	119
---	8000	550	---	230	0.22	0.04	ethanol	10^{-3}	123
---	8000	600	---	230	0.35	0.06	ethanol	10^{-3}	124
800-1500	3000-4000	1 500	590	---	15	1.0	methanol	10^{-4}	25
800-1500	3000-4000	1 090	590	---	12	1.1	methanol	10^{-4}	25
200-300	500-2500	---	570-620	22	---	---	ethanol	4×10^{-5}	61
10	50	---	599	0.026	---	---	ethanol	10^{-3}	23
---	500	100	595	---	0.400	0.4	ethanol	5×10^{-4}	118
---	---	50 000	---	---	400	0.8	ethanol	2.2×10^{-5}	122
<5	700	5.6[b]	587.5	---	0.2	---	methanol	10^{-3}	21

[a]Electrical energy input to flashlamp.

[b]Energy of CO_2 laser pulse.

between the dye channel and the flashlamp annulus, through which a coolant can be flowed.[5,101,1] The annulus also inhibits the propagation of a shock wave, but the temperatures of the coolant and dye solutions must be matched before they enter the laser tube, or thermal inhomogeneities will result.[130] The addition of an appropriate dye to the coolant to provide fluorescence conversion of the flashlamp output to absorption wavelengths of the laser dye increases efficiencies[69] and changes the spectral distribution.[120] Water, as a solvent, minimizes thermally induced inhomogeneities.[93] However, water cannot be used with all dyes.

Flashlamp pumping gives a laser output shifted toward the red from the output for the same dye with laser pumping.[30]

A xenon plasma produced by a CO_2 laser had been used to pump p-terphenyl and rhodamine-6G.[21] The high spectral radiance and fast risetimes of plasmas may allow pumping of uv dyes that cannot be pumped by flashlamps.

Fixed-frequency lasers with proper wavelengths are used to pump dye lasers. Doubled[41,64,66,71,131] and undoubled ruby,[31,132-134] doubled[29,81] and tripled Nd:YAG,[24] doubled Nd:glass,[33,135] GaAlAs diode,[136] nitrogen,[2,22,106,137-151] argon-ion,[53,152,153] xenon-ion[154] and dye[155] lasers have been used. More recently, a KrF laser has been used to pump dyes in the ultraviolet. Different lasers impart different characteristics to the dye-laser output. The polarization of dye-laser output is affected by the nature of the optical pumping source. Pumping intensity also affects polarization,[156] but does not affect the wavelength of dye-laser output.[38] Higher pumping powers increase light-to-light conversion efficiency.[2] Table VI lists some performance characteristics for pumping with various lasers.

Although laser pumping can give light-to-light conversion efficiencies as high as 50%, the net efficiency for conversion of electrical energy into light energy has been higher for flashlamp-pumped dye lasers, because the laser pump sources have generally been relatively inefficient.

Optical Cavity Design

The optical cavity provides the feedback that controls the laser output. Its optical elements can vary widely. Superradiant emission depends only on the medium and its container.[41] Both superradiance and laser action may occur simultaneously.[157] The properties of the output can be controlled by the insertion of mirrors, prisms, gratings, and electro-optical and acousto-optical elements. The tunability of dye lasers results from the broad-band

TABLE VI

DYE-LASER CHARACTERISTICS WITH OPTICAL PUMPING BY OTHER LASERS

Dye	Solvent	Molarity	Pumping Energy (J)	Repetition Rate (Hz)	Output Wavelength (nm)	Output Energy (J)	Efficiency (%)	Ref.
Nd:YAG laser, third harmonic								
POPOP[a]	toluene	5×10^{-4}	5×10^{-4}	50	415-430	1×10^{-6}[b]	0.2	24
DAMC[c]	ethanol	2×10^{-4}	5×10^{-4}	50	440-490	7×10^{-6}[b]	1.4	24
4-methylumbelliferone	water (NaOH)	5×10^{-3}	5×10^{-4}	50	442-467	6×10^{-6}[b]	1.2	24
MADC[d]	ethanol (HCl)	2×10^{-3}	5×10^{-4}	50	430-520	6×10^{-6}[b]	1.2	24
Ruby laser, second harmonic mode-locked								
POPOP[a]	toluene	---	0.08	e	420	---	>10	41
DAMC[c]	ethanol	---	0.08	e	450	---	>10	41
4-methylumbelliferone	basic	---	0.08	e	455	---	>10	41
rhodamine-6G	methanol	---	0.08	e	570	---	>10	41
7-hydroxycoumarin	water (pH 9)	---	0.08	e	470	---	---	41
fluorescein	methanol	---	0.08	e	530	---	---	41
Argon ion laser								
rhodamine-6G + Ammonyx LO[f]	water	2×10^{-4}	---	cw	590	150 mW		53
					594.2	148 mW	25	
					597.4	141 mW	16.4	
Ruby laser, Q-switched								
1,1'-diethyl-4,4'-quinotricarbocyanine iodide	acetone	1×10^{-3}	0.625	---	970-1125	0.03[b]	4.8	31
	DMSO[g]	2.5×10^{-3}	0.625	---	1020-1145	0.0625[b]	10	31
1,1'-diethyl-13-acetoxy-2,2'-quinotetracarbocyanine iodide	DMSO[g]	1.4×10^{-3}	0.625	---	1020-1140	0.035	5.6	31
Nd:YAG laser oscillator-amplifier chain, second harmonic								
disodium fluorescein	methanol	4×10^{-3}	---	10	547-564	0.068	29	29
rhodamine-6G	ethanol	1.1×10^{-4}	---	10	562-576	0.140	51	29
acridine red	methanol	1.6×10^{-4}	---	10	578-594	0.105	44	29
rhodamine-B	methanol	1.4×10^{-4}	---	10	586-598	0.118	48	29
	ethylene glycol	2×10^{-4}	---	10	599-611	0.114	48	29
cresyl violet perchlorate	methanol	2.5×10^{-4}	---	10	642-652	0.102	43	29
	DMSO[g]	2.5×10^{-4}	---	10	658-573	0.041	17	29
3,3'-diethyl-2,2'-oxadicarbocyanine iodide (DODC) + rhodamine-B	methanol	5×10^{-5} 1×10^{-4}	---	10	628-638	0.080	33	29
cresyl violet perchlorate +rhodamine-b	methanol	1.7×10^{-4} 8×10^{-5}	---	10	632-644	0.102	43	29
Xenon-dye laser								
rhodamine-6G	Water	5×10^{-4}	4.5×10^{-5}	120	---	1.8×10^{-6}	4	154
+5% ammonyx LO			6.75×10^{-5}	120	---	3.6×10^{-6}	5.3	154
cresyl violet	ethanol		4.5×10^{-5}	120	---	3×10^{-6}	6.7	154
			6.75×10^{-5}	120	---	6×10^{-6}	8.9	154
Rhodamine-6G dye laser								
cresyl violet	---	---	0.600	---	---	0.100	16.7	155

TABLE VI (continued)

Dye	Solvent	Molarity	Pumping Energy (J)	Repetition Rate (Hz)	Output Wavelength (nm)	Output Energy (J)	Efficiency (%)	Ref.
Giant-pulse, single-mode ruby laser								
3,3'-dimethyl-2,2'-oxatricarbocyanine iodide	acetone	9×10^{-4}	0.45	---	720-750	1.5×10^{-6}	6	133
GaAlAs diode laser								
5,5'-dichloro-11-diphenylamino-3,3'-diethyl-10,12-ethylenethia-tricarbocyanine perchlorate	TMSO[h]	1.4×10^{-3}	---	200	985	---	2.4	136
Nitrogen laser								
PBD	toluene	5×10^{-3}	0.00185	2	357-376	---	~20%	2
BBD	dioxane	2×10^{-3}	0.00185	2	372-405	---	~20%	2
POPOP	dioxane	2×10^{-3}	0.00185	2	415-448	---	~20%	2
DAMC	ethanol	2×10^{-3}	0.00185	2	438-491	---	---	2

[a] 1,4-di(2-phenyloxazolyl)benzene.

[b] pulse length assumed the same as pumping pulse.

[c] 7-diethylamino-4-methylcoumarin.

[d] 7-methylamino-4,6-dimethylcoumarin.

[e] train of pulses lasting ~ 90 ns; separated by 7.4 ns.

[f] 1.5%; surfactant.

[g] dimethyl sulfoxide.

[h] tetramethylene sulfoxide.

fluorescence of organic compounds; the method of tuning is to alter the optical properties of the cavity to obtain the desired frequency.

Many configurations are possible for dye cells. The t most common are a long cell, which will ma. ze gain, and a short cell with minimal surface area, which will maximize energy density. The long cell is commonly used for unspecialized applications. With coaxial-flashlamp pumping, the cell is in the form of a long cylinder; with laser pumping, a rectangular prism may be used. The light from the pump laser is focused by a cylindrical lens into a line the length of the dye cell, transverse to the direction of dye-laser output. Occasionally, a longitudinal pumping arrangement has been used.[48,71,76,131,133,151] Longitudinal pumping has lengthened dye laser pulses in a case of pumping by a modelocked ruby laser.[41] It causes greater excited-state absorption losses than transverse pumping.[14]

Higher energy densities are necessary for pumping some dyes, which are also reported to lower the lasing threshold.[23,124] High energy densities are necessary for cw lasers. Their dye cells are small, with circulation of the dye through the cell. In the cw dye laser, the pump-laser light is focused to a point.[53] Focusing to a point is also desirable for superradiance.[41] For power outputs greater than 1 W, the pumping intensity required for cw dye lasers is high enough to damage the windows of the dye cell. A free jet stream of the dye solution flowing through the resonator of the laser has been used to eliminate this problem. The jet stream must have an optical quality similar to that of other laser components, so that the flow properties

are critical to its operation. Thickness fluctuations have been investigated for jet-stream lasers, and linewidths have been found to be comparable to those of other cw dye lasers.[158] Jet-stream cw dye lasers have been used for high-resolution spectroscopy.[153]

Waveguide dye lasers have very narrow dye channels to take advantage of focusing and refraction of the laser beam by refractive-index gradients in the dye solution and by reflection from the walls of the channel.[136,144,159] They may be constructed with thick films of polymer containing a dye and deposited on a substrate with a refractive index greater than that of the polymer.[160] High-output energies, good efficiencies, and long pulses have been reported for waveguide dye lasers.[136,159,161] Waveguide lasers can be tuned by alteration of the channel thickness.[144] Reference 162 reviews waveguide dye lasers.

The simplest arrangement of optical elements outside the dye cell consists of one mirror on each end of the dye cell, one of which is partially transmitting to allow for output. The mirrors may be planar or curved. Both distance from the dye cell and reflectivity of the output coupler affect the output power.[142,152] Glass-fiber bundles have also been used to provide feedback and output.[163]

For tuning the wavelength of the laser light, a wavelength-selective element must be included in the cavity. Gratings are commonly used,[5,30,61,139,143,150] but their losses may be too high for high photon fluxes, which may be necessary for photochemistry applications. Prisms can be used and will allow for higher photon fluxes than gratings.[24] More than one prism is usually needed to produce sufficient dispersion for satisfactory tuning.[164,165] An array of prisms has been used in a ring configuration giving greater control of mode structure and allowing for traveling-wave operation.[145,166] An oscillator-amplifier combination of two dye lasers has been used, in which the oscillator is tuned with a diffraction grating and the power is generated in the amplifier, to compensate for the low power densities required by the diffraction grating.[132] Tuning has also been accomplished in a superradiant laser by use of a wedge-shaped dye cell, which can be moved to give a continuous change of path length.[134] Fabry-Perot etalons,[36,128,147,167] acousto-optic filters,[168,169] electro-optic filters,[152] Christiansen filters,[170] and thin nitrocellulose membranes (pellicles) either coated with multilayer dielectrics or uncoated[171] have been used for tuning. The method of tuning affects the laser characteristics; for example, the pumping threshold for rhodamine-6G tuned with a grating was 15 J, but was 22 J with a prism.[61]

The output frequency can be stabilized by locking to a stable reference.[153,172-174] Dye lasers stabilized in this way have been used for ultraprecise spectroscopy.

Extremely short pulses (picosecond duration) can be obtained from dye lasers by pumping with a modelocked laser[32,41,175] or by passive modelocking with an appropriate dye solution.[32,41,175] Pumping sources for passive modelocking are generally cw dye lasers, but the possibility of passive modelocking with flashlamp-pumping has been investigated analytically.[176] Repetition rates of up to 10^5 Hz have been obtained with peak pulse powers of several kilowatts (energies of several nanojoules).[177] An extensive review literature exists on the theory and practice of modelocking.[178-181]

Another technique for the production of subnanosecond pulses with high repetition rates is to make use of resonator transients that result from an interaction between an excess population inversion and photons within the cavity.[150] Pulses of 600 to 900 ps have been obtained from rhodamine-6G, disodium fluorescein, and two coumarins by pumping with a nitrogen laser.

Multiple-wavelength operation, of interest mainly in holography, can be

obtained in several ways. Several aligned cells can be pumped simultaneously by a nitrogen laser.[138] Acousto-optic beam deflectors,[139] composite holographic diffraction gratings,[28,182] coupled cavities with different dyes,[104,148] multiple-dye jet streams,[183] and Fabry-Perot etalons[128] have been used.

Feedback within a dye solution can be substituted for external mirrors.[184] A nonlinear self-induced mirror has been formed in the laser solutions;[185] the addition of a cholesteric liquid crystal also gives internally distributed feedback.[186]

The design of the optical cavity and the method of tuning also affect threshold energies,[61,187] pulse length,[188] mode selection,[140] suppression of background fluorescence,[189] and structure in the emission spectrum.[135]

Dye Laser Efficiency - Wavelength Relationships

Dye-laser efficiency cannot be related to wavelength by a simple relationship. Each dye has its own characteristic tunability range and emission efficiency. The laser emission efficiency varies over the range of tunability.

Statements have been made to the effect that tuning methods do not decrease output power of the laser.[10,17] For example, C. V. Shank[10] states, "With the insertion of frequency selective elements into the optical cavity, the bandwidth of oscillation can be reduced to a small fraction of an angstrom without appreciable loss in power." In other words, the integral under the output curve for broad-band oscillation (Fig. 3) may be only slightly greater than the integral under the output curve for tuned oscillation. At an upper limit on tuned output efficiency, the integrals are the same.

The configuration of the optical cavity has a strong effect on efficiency. Results obtained with one laser configuration may not be reproducible in another.

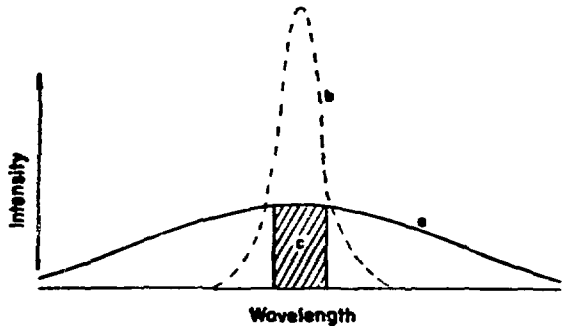

Fig. 3. Spectral condensation Curve a represents the broadband output of a dye laser without tuning. Curve b is the output with tuning. Area c might be expected without feedback.

Absorption of pumping radiation is another major factor affecting the efficiency of dye lasers. Obvicusly, only the radiation that is absorbed can produce the necessary inversion for lasing. Because a strong singlet-singlet absorption is characteristic of laser dyes, there is an optimum wavelength range for absorption of pump radiation by laser dyes.

Because flashlamps have a broad-band output, the use of fluorescence converters in flashlamp-pumped dye lasers to convert light at unusable wavelengths to wavelengths in the absorption band of the dye can improve efficiencies. Many variations on this method are possible, which were discussed in the section on Dye Characteristics.

The emission spectrum of a dye is nearly a mirror image of the absorption spectrum, separated from it by the Stokes shift. The dye is generally tunable over the range of the emission spectrum. However, the emission spectrum alone does not determine the efficiency of laser output. Other factors, such as radiationless decay, excited-state absorption, and nonlinear effects enter into the efficiency. Some of these effects have been studied analytically.[42] The complexity of these interactions is discussed in Ref. 58. The

relative positions of the emission and the excited-state absorptions are different for different dyes. These relationships have been studied systematically by Pavlopoulos and Hammond,[55,56] who conclude that more efficient laser dyes will probably be developed.

In a given liquid-dye laser, the relationship between light-to-light energy conversion efficiency and wavelength can be quite complex. Figure 4 gives the wavelength-efficiency relationship for a cw dye laser.[54] Figure 5 shows power ratios for selected dyes in the uv and blue. These power ratios are equal to the efficiencies if the durations of the input and output pulses are the same; they are equivalent to relative efficiencies if these durations differ but the pulse lengths are the same for different dyes. Selected values of efficiency from Table VI are plotted in Fig. 6 as a function of wavelength.

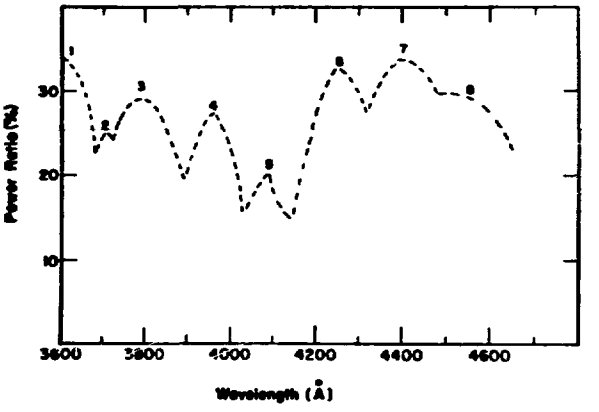

Fig. 5. Relative power ratios for several dyes in a N_2 laser pumped dye laser between 3600 Å and 4600 Å. (1) butyl-PBD in toluene, (2) PPF in toluene, (3) BBD in toluene, (4) -NND in toluene, (5) BBD in toluene (74%) and POPOP in p-dioxane (26%). (6) POPOP in p-dioxane, (7) dimethyl-POPOP in p-dioxane, (8) coumarin 120 in ethanol.

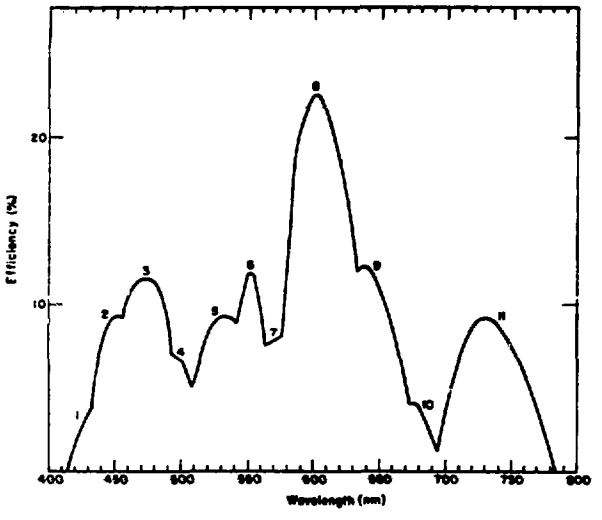

Fig. 4. Efficiency:wavelength relationship for a dye laser using different dyes between 420 and 760 nm; (1) carbostyril 165, (2) coumarin 2, (3) 7-dimethyl amino-4-methyl coumarin, (4) coumarin 102, (5) coumarin 7, (6) sodium fluorescein, (7) rhodamine-110, (8) rhodamine-6G, (9) rhodamine-B, (10) cresyl violet perchlorate, (11) nile blue-A perchlorate.

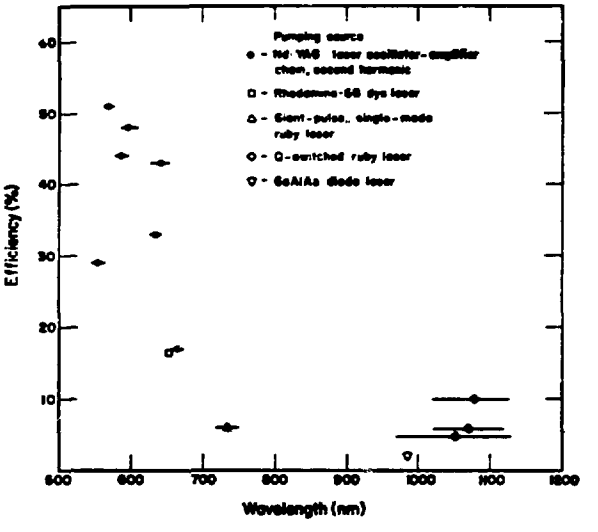

Fig. 6. Efficiency:wavelength relationships for selected dye lasers.

REFERENCES

1. D. Basting, F. P. Schafer, and B. Steyer, "New Laser Dyes," Appl. Phys. 3, 81-8 (1974).

2. M. Maeda and Y. Miyazoe, "Efficient Ultraviolet Organic Liquid Laser Pumped by a High Power Nitrogen Laser," Japan. J. Appl. Phys. 13(5), 827-34 (1974).

3. G. A. Abakumov, V. V. Fadeev, R. V. Khokhlov, and A. P. Simonov, "UV Dye Lasers," Spectrosc. Lett. 8(9), 651-67 (1975).

4. J. P. Webb, F. G. Webster, and B. E. Plourde, "Sixteen New IR Laser Dyes," IEEE J. Quantum Electron. 11(3), 114-20 (1975).

5. J. B. Marling, J. G. Hawley, E. M. Liston, and W. B. Grant, "Lasing Characteristics of Seventeen Visible-Wavelength Dyes Using a Coaxial-Flashlamp-Pumped Laser," Appl. Opt. 13(10), 2317-20 (1974).

6. F. P. Schafer, editor, Dye Lasers (Springer-Verlag, New York, 1973).

7. B. B. Snavely, "Flashlamp-Excited Organic Dye Lasers," Proc. IEEE 57(8), 1374-90 (1969).

8. M. J. Wilkes, C. R. Pidgeon, and S. D. Smith, "Tunable Lasers," Phys. Bull. 24 (July), 319-21 (1973).

9. R. S. Keller, "Tunable Lasers for Chemists," ChemTech 1973(10), 626-34.

10. C. V. Shank, "Physics of Dye Lasers," Rev. Mod. Phys. 47(3), 649-57 (1975).

11. J. Kuhl and W. Schmidt, "Tunable Coherent Light Sources," Appl. Phys. 3, 251-70 (1974).

12. D. E. Evans, J. Puric, and M. L. Yeoman, "Quenching of Laser Action in Cresyl Violet by 6943 Å Radiation," Appl. Phys. Lett. 25(3), 151-2 (1974).

13. E. Sahar and I. Wieder, "Absorption Cross Sections of the First Excited Singlet State of Laser Dyes at 3371 Å," IEEE J. Quantum Electron. 10, 612-14 (1974).

14. J. Shah and R. F. Leheny, "Excited-State Absorption Spectrum of Cresyl Violet Perchlorate," Appl. Phys. Lett. 24(11), 562-4 (1974).

15. J. Faure, J. -P. Fouassier and D. -J. Lougnot, "$S_1 \rightarrow S_n$ Absorption Cross Sections of Laser Dyes at 347 nm and 694 nm," Phys. Lett. 50A(5), 319-20 (1974).

16. S. Speiser, "Photoquenching II. Pulsed-Laser-Pumped Dye Laser Systems," Chem. Phys. 6, 479-83 (1974).

17. P. P. Sorokin, J. R. Lankard, V. L. Moruzzi, and E. C. Hammond, "Flashlamp-Pumped Organic Dye Lasers," J. Chem. Phys. 48(10), 4726-41 (1968).

18. Yu. I. Lifanov, V. A. Kuz'min, A. K. Chibisov, I. I. Levkoev, and A. V. Karyakin, "Processes of the Radiationless Deactivation of Excited Molecules of Polymethine Dyes," Zh. Prikl. Spektrosk. 20(2), 221-4 (1974).

19. C. P. Kezthelyi, "Chemistry in Lasers. I. The Role of the Stokes 0-0 Loss," Spectrosc. Lett. 7(1), 19-25 (1974).

20. C. P. Kezthelyi, "Chemistry in Lasers. II. Contribution from Precursor States A Comparison of the Time Evolution of Electronically Excited States Under Spontaneous and Stimulated Emission Conditions," Spectrosc. Lett. 7(1), 27-32 (1974).

21. W. T. Silfvast and O. R. Wood II, "3500-Å p-Terphenyl Dye Laser Pumped by a CO_2-Laser-Produced Plasma," Appl. Phys. Lett. 25(8), 447-9 (1975).

22. P. W. Smith, P. F. Liao, C. V. Shank, T. K. Gustafson, C. Lin and P. J. Maloney, "Optically Excited Organic Dye Vapor Laser," Appl. Phys. Lett. 25(3), 144-6 (1974).

23. M. Maeda and Y. Miyazoe, "A Compact Flashlamp-Pumped Dye Laser with Fast Flash Risetime," Japan. J. Appl. Phys. 13(2), 369-70 (1974).

24. M. Okada, S. Shimizu, and S. Terri, "Dye Laser Pumped by the Third Harmonic of Nd YAG Laser," Japan J. Appl. Phys. 12, 1284-5 (1973).

25. M. I. Dzyubenko, I. G. Naumenko, V. P. Polipenko, and S. E. Soldatenko, "High-Efficiency Visible-Band Laser Using Dyes," Zh. Eksp. Teor. Fiz. Pis. Red. 18(1), 43-6 (1973).

26. P. R. Hammond, A. N. Fletcher, R. A. Henry, R. L. Atkins, and D. W. Moore, "Near Ultraviolet Lasing Dyes," Naval Weapons Center report NWC TP 5708, Part I (September 1975).

27. E. J. Schimitschek, J. A. Trias, M. Taylor, and J. E. Celto, "New Improved Laser Dye for the Blue-Green Spectral Region," IEEE J. Quantum Electron. 9 781-2 (1973).

28. A. A. Freisem, U. Ganiel, G. Neumann, and D. Peri, "A Tunable Dye Laser with a Composite Holographic Wavelength Selector," Opt. Commun. 9(2), 149-51 (1973).

29. E. O. Ammann, C. D. Decker, and J. Falk, "High-Peak-Power 532-nm Pumped Dye Laser," IEEE J. Quantum Electron. 10, 463-5 (1974)

30. A. Hirth, K. Vollrath, J. Faure, and D. Lougnot, "Flashlamp-Excited Dye Lasers in the Near Infrared," Opt. Commun. 7(4), 339-42 (1973).

31. H. Lotem, "A Tunable Dye Laser in the Range 1.0-1.145 μm," Opt. Commun. 9(4), 346-7 (1973).

32. B. S. Neporent, V. V. Kryukov, G. V. Lukomskii, and V. B. Shilov, "Spectral-Time Characteristics of Dye-Solution Lasing in Pumping with a Series of Ultrashort Pulses," Opt. Spektrosk. 35, 531-4 (1973).

33. B. S. Neporent, V. B. Shilov, and G. V. Lukomskii, "Spectral Kinetics of the Laser Action in Solutions of Various Organic Substances," Opt. Spektrosk. 35, 535-9 (1973).

34. B. S. Neporent, V. B. Shilov, and G. V. Lukomskii, "Determination of the Probabilities of Relaxation Processes in Complex Organic Molecules from the Relaxation Shift of Laser Spectra," Opt. Spektrosk. 37, 1186-7 (1974).

35. E. B. Aslanidi, A. I Kurasbediani, B. S. Lezhava, and V. V. Mumladze, "Effect of Solvent on the Nonlinear Properties of Solutions of Organic Dyes," Opt. Spektrosk. 37, 482-6 (1974).

36. J. B. Atkinson and F. P. Pace, "The Spectral Linewidth of a Flashlamp-Pumped Dye Laser," IEEE J. Quantum Electron. 9(6), 569-74 (1973).

37. K. G. Breitschwerdt, "Frequency Shift of Dye Laser Emission in the Linear Approximation," Phys. Lett. 43A(6), 515-16 (1973).

38. A. N. Rubinov, V. A. Batyrev, and T. Sh. Efendiev, "Kinetics of the Lasing Spectrum of Organic Dye Solutions," Zh. Prikl. Spektrosk. 18(5), 806-12 (1973).

39. A. Baczynski, T. Marszalek, H. Walerys, and B. Zietek, "The Influence of Molecular Parameters on Laser Properties of Dye Solutions," Acta Phys. Polon. A44(6), 805-12 (1973).

40. A. M. Bonch-Bruevich, T. K. Razumova, and I. O. Starobogatov, "Studies on the Character of Broadening of the Energy States of Polymethine Dye Solutions," Opt. Spektrosk. 35, 640-5 (1973).

41. C. Lin, T. K. Gustafson, and A. Dienes, "Superradiant Picosecond Laser Emission from Transversely Pumped Dye Solutions," Opt. Commun. 8(3), 210-15 (1973).

42. B. I. Stepanov and V. A. Batyrev, "Tuning of Organic Lasers," Opt. Spektrosk. 37, 166-70 (1974).

43. G. Mourou, "Spectral Hole Burning in Dye Solutions," IEEE J. Quantum Electron. 11(1), 1-8 (1975).

44. D. W. Vahey and A. Yariv, "Effects of Spectral Cross Relaxation and Collisional Dephasing on the Absorption of Light by Organic-Dye Solutions," Phys. Rev. A10(5), 1578-90 (1974).

45. D. W. Phillion, D. J. Kuizenga, and A. E. Siegman, "Rotational Diffusion and Triplet State Processes in Dye Laser Solutions," J. Chem. Phys. 61(9), 3828-39 (1974).

46. A. M. Bonch-Bruevich, T. K. Razumova and G. M. Rubanova, "Induced Absorption of Polymethine Dye Solutions," Opt. Spektrosk. 35, 832-40 (1973).

47. F. P. Schafer and L. Ringwelski, "Triplet Quenching by Oxygen in a Rhodamine 6G Laser," Z. Naturforsch., Teil A 28(5), 792-3 (1973).

48. R. F. Leheny and J. Shah, "Amplification and Excited State Absorption in Longitudinally Pumped Laser Dyes," IEEE J. Quantum Electron. 11(2), 70-4 (1975).

49. R. B. Schaefer and C. R. Willis, "Effects of Triplet State Losses on Coherent Properties of Organic Dye Lasers," Phys. Lett. 48A(6), 465-6 (1974).

50. J. Kleinschmidt, W. Tottleben, and S. Rentsch, "Measurements of Two Photon Absorption in the Cavity of an Organic Dye Laser," Exp. Tech. Phys. 22(3), 191-5 (1974).

51. R. Konjevic, J. Jovicic, N. Konjevic, and L. Cirkovic, "Time Resolved Spectroscopy of Rhodamine Dye Laser," Fizika 5, 17-26 (1973).

52. A. Hirth, J. Faure, and D. Lougnot, "Quenching Effects in Flashlamp-Excited Polymethine Dye Lasers," Opt. Commun. 8(4), 318-22 (1973).

53. R. R. Jacobs, A. Lempicki, and H. Samelson, "Efficient and Damage-Resistant Tunable CW Dye Laser," J. Appl. Phys. 44(6), 2775-80 (1973).

54. J. M. Yarborough, "CW Dye Laser Emission Spanning the Visible Spectrum," Appl Phys. Lett. 24(12), 629-30 (1974).

55. T. G. Pavlopoulous, "Prediction of Laser Action Properties of Organic Dyes from their Structure and the Polarization Characteristics of their Electronic Transitions," IEEE J. Quantum Electron. 9, 510-16 (1973).

56. T. G. Pavlopoulos and P. R. Hammond, "Spectroscopic Studies of Some Laser Dyes," J. Amer. Chem. Soc. 96(21), 6568-79 (1974).

57. V. A. Mostovnikov, A. N. Rubinov, M. A. Al'perovich, V. I. Avdeeva, I. I. Levkoev, and M. M. Loiko, "Dependence of the Luminescence and Generation Properties of Solutions of Polymethine Dyes on their Structure," Zh. Prikl. Spektrosk. 20(1), 42-7 (1974).

58. J. Langelaar, "Use of Time-Resolved Excited State Spectroscopy for Selection of Laser Dyes," Appl. Phys. 6, 61-4 (1975).

59. K. Takahashi and H. Kusakawa, "Solvent Effect on Wavelength of Stimulated Emission from Dye Laser," Mitsubishi Denki Giho 48(5), 646-9 (1974); Chem. Abstr. 81, 97567y (1974).

60. L. G. Pikulik, A. I. Maksimov, and K. I. Rudik, "A Study of the Polarization of Stimulated Emission from Solutions of Phthalimides," Zh. Prikl. Spektrosk. 19(5), 1025-9 (1973).

61. K. H. Drexhage, "Laser Media Containing Fluorinated Alcohols," U.S. Patent 3,736,524 (May 1973); Chem. Abstr. 79, 47750r (1973).

62. V. I. Studenov and N. G. Bakhshiev, "Intermolecular Interactions and the Stimulated Emission Spectra of Activated Liquid Systems. 3," Opt. Spektrosk. 36, 392-7 (1974).

63. I. B. Naumenko, A. M. Korobov, and M. I. Dzyubenko, "Lasing Characteristics of Dye Solutions in Dispersive Cavities Under Lamp Pumping," Opt. Spektrosk. 34, 1175-80 (1973).

64. M. Nakashima, R. C. Clapp, and J. A. Sousa, "Benzocoumarins, a New Family of Laser Dyes," Nature Phys. Sci. 245, 124-6 (1973).

65. M. Takakusa and T. Itoh, "Extended Tunability of a 4-MU Dye Laser Obtained in an Alcoholic Solution Containing a Small Amount of Water," Opt. Commun. 10(1), 8-10 (1974).

66. A. Bergman and J. Jortner, "Study of Spontaneous and Stimulated Emission of Various Solutions of 4-Methylumbelliferone," J. Lumin. 6, 390-403 (1973).

67. J. M. Drake, E. M. Tam, and R. I. Morse, "The Use of Light Converters to Increase the Power of Flashlamp-Pumped Dye Lasers," IEEE J. Quantum Electron. 8, 92-4 (1972).

68. J. Weber, "Waveguide Dye Lasers Prepared by Diffusion," Opt. Commun. 8(4), 316-7 (1973).

69. S. Reich and G. Neumann, "Photobleaching of Rhodamine 6G in Polyacrylonitrile Matrix," Appl. Phys. Lett. 25(2), 119-21 (1974).

70. B. Steyer and F. P. Schafer, "A Vapor-Phase Dye Laser," Opt. Commun. 10(3), 219-20 (1974).

71. N. A. Borisevich, I. I. Kalosha, and V. A. Tolkachev, "Lasing of Complex Organic Molecules in the Gas Phase," Zh. Prikl. Spektrosk. 19(6), 1108-9 (1973).

72. P. W. Smith, P. F. Liao, C. V. Shank, C. Lin, and P. J. Maloney, "The POPOP Dye Vapor Laser," IEEE J. Quantum Electron. 11(2), 84-9 (1975).

73. R. G. Pappalardo and S. A. Ahmed, "Fluorescent Organic Compound Laser," U.S. Patent 3,857,793 (December 1974); Chem. Abstr. 82, 162874h (1975).

74. R. T. Hodgson and S. C. Wallace, "Electron Beam Pumping of Laser Dyes," AD report 778 032 (December 1973).

75. F. P. Schafer, "Exciting Liquid Lasers," U.S. Patent 3,835,417 (September 1974), Chem. Abstr. 82, 178085n (1975).

76. R. Pappalardo, S. L. Shapiro, S. Ahmed, and R. Alfano, "Search for Superradiant Emission from 'Complex' Organic Molecules in the Vapor Phase," J. Chem. Phys. 60(9), 3368-72 (1974).

77. T. Sakurai and H. G. de Winter, "Properties of Rhodamine 6G in Vapor Phase," J. Appl. Phys. 46(2), 875-8 (1975).

78. N. A. Borisevich, "Laser Action of Complex Molecules in the Gas Phase," Spectrosc. Lett. 8(9), 607-20 (1975).

79. O. Teschke and A. Dienes, "Solvent Effects on the Triplet State Population in Jet Stream CW Dye Lasers," Opt. Commun. 9(2), 128-31 (1973).

80. E. N. Antonov, V. G. Koloshnikov, V. R. Mironenko, and D. N. Nikogosyan, "Influence of the Solvent on the Output Parameters of a cw Dye Laser," Kvantovaya Elektron. (Moscow) 1, 204-6 (1974).

81. J. Weber, "Effect of Concentration on Laser Threshold of Organic Dye Laser," Z. Physik 258, 277-83 (1973).

82. I. Ketskemety and L. Kozma, "Some Remarks Concerning the Theory of Quasistationary Dye Lasers," Acta Physica 35(1-4), 63-71 (1974).

83. I. B. Berlman, M. Rokni, and C. R. Goldschmidt, "Lasing in Some Aromatic Couples by Means of Energy Transfer," Chem. Phys. Lett. 22(3), 458-60 (1973).

84. Yu. E. Zabiyakin, V. S. Smirnov, and N. G. Bakhshiev, "Experimental Study of the Lasing Characteristics of Solutions of Phthalimide Substitutes with Lamp Pumping," Opt. Spektrosk. 35, 958-9 (1973).

85. A. Dienes, R. K. Jain, and C. Lin, "Formation Mechanisms in an Excited-State-Reaction Dye Laser," Appl. Phys. Lett. 22(12), 632-4 (1973).

86. R. L. Kohn, C. V. Shank, and A. Dienes, "Observation of Inhomogeneity in the Gain Spectrum of a Coumarin Laser Dye," Opt. Commun. 7(4), 309-12 (1973).

87. M. R. Groves, S. C. Haydon, and O. M. Williams, "The Mechanisms for Dye Laser Fluorescence from 4-Methylumbelliferone," Opt. Commun. 9(1), 42-7 (1973).

88. Y. Aoyagi and S. Namba, "Temperature Tuning of 4-Methylumbelliferone Dye Laser," Japan. J. Appl. Phys. 12(4), 624-5 (1973).

89. A. Dienes, C. V. Shank, and R. L. Kohn, "Characteristics of the 4-Methylumbelliferone Laser Dye," IEEE J. Quantum Electron. 9(8), 833-43 (1973).

90. A. W. H. Mau, "Broadband Tunability of Dye Lasers," Opt. Commun. 11(4), 356-9 (1974).

91. R. K. Bauer, A. Kowalczyk, and M. Berndt, "Influence of Water on the Exciplex Formation of 4-Methylumbelliferone," Bull. Acad. Polon. Sci. 22(6), 637-41 (1974).

92. M. V. Belokon', A. N. Rubinov, and V. S. Strizhnev, "Lasing by Aqueous Rhodamine 6G with Detergents and Lamp Excitation," Zh. Prikl. Spektrosk. 19(1), 39-43 (1973).

93. V. S. Smirnov, Yu. E. Zabiyakin, and N. G. Bakhshiev, "Laser Action in Solutions of Rhodamine 6G in Mixed Aqueous-Organic Solvents," Opt. Spektrosk. 38, 591-4 (1975).

94. J. Ferguson and A. W. -H. Mau, "Spontaneous and Stimulated Emission from Dyes. Spectroscopy of the Neutral Molecules of Acridine Orange, Proflavine, and Rhodamine B," Aust. J. Chem. 26, 1617-24 (1973).

95. M. I. Snegov, I. I. Reznikova, and A. S. Cherkasov, "Nature of the Shift in the Absorption and Fluorescence Spectra of some Rhodamines on Variation of their Concentration in Solution and the Acidity of the Solvent," Opt. Spektrosk. 36 96-9 (1974).

96. R. Srinivasan, R. J. VonGutfeld, C. S Angadiyavar, and R. W. Dreyfus, "Anomalous Fluorescence and Laser Emission from 7-Alkylamino Coumarins in Acid Solutions," Chem. Phys. Lett. 25(4), 537-40 (1974).

97. C. E. Hackett and C. F. Dewey, Jr., "Improved Temporal Stability of Polymethine Laser Dyes in Aqueous Solutions," IEEE J. Quantum Electron. 9, 119-20 (1973).

98. S. L. Chin, "Further Evidence of Dimer Emission from Superradiant Travelling Wave Laser of Concentrated Aqueous Solution of Rhodamine 6G and B," Phys. Lett. 48A(6), 402-4 (1974).

99. M. V. Melishchuk, E. A. Tikhonov, and N. T. Shpak, "Generation of Stimulated Emission by Great Molecules at Low Temperatures," Spectrosc. Lett. 8(9), 669-84 (1975).

100. J. G. Calvert and J. N. Pitts, Jr., Photochemistry, (John Wiley & Sons, New York, 1966).

101. J. Jethwa and F. P. Schafer, "A Reliable High Average Power Dye Laser," Appl. Phys. 4, 299-302 (1974).

102. M. B. Levin, A. S. Cherkasov, and V. I. Shirokov, "Use of Luminescence Converter in a Lamp Laser Based on Rhodamine 6G in Ethanol," Opt. Spektrosk. 38, 595-8 (1975).

103. G. Marowsky and F. Zaraga, "Dual-Wavelength Operation of Two Coupled Dye Lasers," Opt. Commun. 11(4), 343-5 (1974).

104. M. I. Dzyubenki, A. Ya. Matveev, and I. G. Naumenko, "Gain in the Output Efficiency of Lasers Based on Organic Dye Solutions," Opt. Spektrosk. 37, 745-9 (1974).

105. R. C. Wilborn and H. C. Brayman, "Simultaneous Two-Wavelength Output from Multiple-Dye Pulsed Tunable Dye Lasers," J. Appl. Phys. 45(11), 4912-14 (1974).

106. A. Dienes and M. Madden, Jr., "Study of Excitation Transfer in Dye Mixtures by Measurements of Gain Spectra," J. Appl. Phys. 44(9), 4161-4 (1973).

107. C. Lin and A. Dienes, "Study of Excitation Transfer in Laser Dye Mixtures by Direct Measurement of Fluorescence Lifetime," J. Appl. Phys. 44(11), 5050-2 (1973).

108. B. S. Neporent and A. G. Makogonenko, "On the Mechanism of 'Hole Burning' in Vibronic Spectra of Complex Organic Compounds," Spectrosc. Lett. 8(9) 711-18 (1975).

109. A. V. Aristov, E. N. Viktorova Yu. S. Maslyukov, I. I. Reznikova, and A. S. Cherkasov, "Effect of the Structure and Degree of Purification of Rhodamines on Their Generating Characteristics During Lamp Pumping," Zh. Prikl. Spektrosk. 19(2), 250-3 (1973).

110. B. H. Winters, H. I. Mandelberg, and W. B. Mohr, "Photochemical Products in Coumarin Laser Dyes," Appl. Phys. Lett. 25(12), 723-5 (1974).

111. F. Pinter, I. Ketskemety, E. Farkash, and L. Kozma, "Effect of Photodecay on the Generation of a Dyestuff Laser with Lamp Pumping," Zh. Prikl. Spektrosk. 19(2), 246-9 (1973).

112. J. Weber, "Continuously UV-Bleaching of Organic Laser Dyes," Phys. Lett. 45A(1), 35-6 (1973).

113. J. Weber, "Study of the Influence of Triplet Quencher on the Photobleaching of Rhodamine 6G," Opt. Commun. 7(4), 420-2 (1973).

114. A. V. Aristov and Yu. S. Maslyukov, "Amplification and Induced Absorption in Solutions of Organic Luminophors," Opt. Spektrosk. 35, 1138-41 (1973).

115. E. J. Schmitschek, J. A. Trias, P. R. Hammond, and R. E. Atkins, "Laser Performance and Stability of Fluorinated Coumarin Dyes," Opt. Commun. 11(4), 352-5 (1974).

116. V. V. Gruzinskii, N. M. Paltarak, and P. I. Petrovich, "Generation from Solutions of Some Organic Compounds in the Blue Spectral Region," Zh. Prikl. Spektrosk. 19(2), 352-7 (1973).

117. A. Hirth, K. Vollrath, and J. P. Fouassier, "Optimizing the Emission Characteristics of a Rhodamine 6G Dye Laser," Opt. Commun. 9(2), 139-45 (1973).

118. T. Morrow and H. T. W. Price, "A Simple Reliable Co-Axial Dye Laser System," Opt. Commun. 10(2), 133-6 (1974).

119. R. Konjevic and N. Konjevic, "Coaxial Glass Flashlamp for Organic Dye Laser," Fizika 5, 49-51 (1973).

120. R. Konjevic and N. Konjevic, "Coaxial Glass Flashlamp and Dye Laser System," Fizika 6, 61-5 (1974).

121. F. N. Baltakov, B. A. Barikhin, and L. V. Sukhanov, "*Spatial and Temporal* Characteristics of a 100 J Laser Using a Solution of Rhodamine 6G in Ethanol," Kvantovaya Elektron. 1, 973-7 (1974).

122. F. N. Baltakov, B. A. Barikhin, and L. V. Sukhanov, "400-J Pulsed Laser Using a Solution of Rhodamine 6G in Ethanol," Zh. Eksp. Teor. Fiz. Pis. Red. 19, 300-2 (1974).

123. R. L. St. Peters and D. J. Taylor, "Face-Pumped High-Average-Power Low-Distortion Dye Laser," Appl. Phys. Lett. 23(2), 90-1 (1973).

124. M. Maeda, Y. Noda, and Y. Miyazoe, "Dye Laser Pumped by a Flashlamp with a Fast Risetime," Kyushu Daigaku Kogaku Shuho 46(6), 708-13 (1973); Chem. Abstr. 80, 114658c (1974).

125. T. F. Ewanizky, R. H. Wright, Jr., and H. H. Thiessing, "Shock-Wave Termination of Laser Action in Coaxial Flash Lamp Dye Lasers," Appl. Phys. Lett. 22(10), 520-1 (1973).

126. P. Burlamacchi, R. Pratesi, and U. Vanni, "Refractive Index Gradient Effects in a Superradiant Slab Dye Laser," Opt. Commun. 9(1), 31-4 (1973).

127. F. Aissenegg and A. Gilly, "On the Construction of a Simple Organic Dye Laser," Acta Phys. Austr. 37, 254-8 (1973).

128. P. Flamant and Y. H. Meyer, "Time-Dependent Intensity Distribution in a Two-Wavelength Dye Laser," Opt. Commun. 13(1), 13-16 (1975).

129. S. G. Varnado, "Degradation in Long-Pulse Dye Laser Emission Under Fast-Flow Conditions," J. Appl. Phys. 44(11), 5067-8 (1973).

130. J. M. Drake and R. I. Morse, "Operating Characteristics of a Linear Flashlamp-Pumped Dye Laser Using a Coaxial Dye Cell," Opt. Commun. 12(2), 132-5 (1974).

131. K. Kato and A. Fujisawa, "A Longitudinally Pumped High-Power Dye Laser in the Blue," Opt. Commun. 10(1), 21-2 (1974).

132. J. L. Carlsten and T. J. McIlrath, "An Oscillator-Amplifier Dye Laser: Tunable High Powers without Grating Damage," Opt. Commun. 8(1), 52-5 (1973).

133. A. Owyoung, "An Efficient Ruby Laser Pumped, Diffraction Limited Dye Laser," Opt. Commun. 11(1), 14-17 (1974).

134. T. A. P. Rao and N. Seetharaman, "Mechanical Tuning of a Superradiant Dye Laser Wavelength," Japan J. Appl. Phys. 13(8), 1329-30 (1974).

135. V. M. Baev, E. A. Sviridenkov, and M. P. Frolov, "*High-Sensitivity Spectroscopy* with the Aid of Dye Lasers," Kvantovaya Elektron. (Moscow) 1, 1245-7 (1974).

136. G. Wang, "Infrared Dye Laser Excited by a Diode Laser," Opt. Commun. 10(2), 149-53 (1974).

137. I. Itzkan, "Transverse-Flowing Liquid Laser," U.S. Patent 3,740,665 (June 1973); Chem. Abstr. 79, 85540e (1973).

138. M. Nakashima and J. A. Sousa, "Polychromatic Pulsed Dye Laser," Spectrosc. Lett. 7(1), 15-17 (1974).

139. L. D. Hutcheson and R. S. Hughes, "Electronic Tuning of a Dye Laser with Simultaneous Multiple-Wavelength Output," IEEE J. Quantum Electron. 10, 462-3 (1974).

140. J. J. Wynne, "Generation of the Rotationally Symmetric TE_{01} and TM_{01} Modes from a Wavelength-Tunable Laser," IEEE J. Quantum Electron. 10(2), 125-7 (1974).

141. R. F. Carsti, "Flowing Liquid Laser," U.S. Patent 3,745,484 (July 1973); Chem. Abstr. 79, 85540e (1973).

142. U. Ganiel and G. Neumann, "Power Output Coupling in a Dye Laser Pumped by a Nitrogen Laser," Opt. Commun. 12(1), 5-7 (1974).

143. F. B. Dunning and R. F. Stebbings, "The Efficient Generation of Tunable and Near UV Radiation Using a N_2 Pumped Dye Laser," Opt. Commun. 11(2), 112-114 (1974).

144. Y. Aoyagi and S. Namba, "Laser Oscillation in Simple Corrugated Optical Waveguide," Appl. Phys. Lett. 24(11), 537-9 (1974).

145. F. Zaraga, "A Single-Mode Nitrogen-Pumped Tunable Dye Ring-Laser," Appl. Phys. 4, 87-8 (1974).

146. M. I. Bell and R. N. Tyte, "Pulsed Dye Laser System for Raman and Luminescence Spectroscopy," Appl. Opt. 13(7), 1610-14 (1974).

147. R. Wallenstein and T. W. Hansch, "Linear Pressure Tuning of a Multielement Dye Laser Spectrometer," Appl. Opt. 13(7), 1625-8 (1974).

148. S. A. Ahmed, J. S. Gergely, and D. Infante, "Energy Transfer Organic Dye Mixture Lasers," J. Chem. Phys. 61(4), 1584-5 (1974).

149. C. Lin, "Near-Infrared Dye Laser Emission from Ultraviolet Nitrogen-Laser-Pumped Dye Solutions," IEEE J. Quantum. Electron. 11(1), 61 (1975).

150. C. Lin and C. V. Shank, "Subnanosecond Tunable Dye Laser Pulse Generation by Controlled Resonator Transients," Appl. Phys. Lett. 26(7), 389-91 (1975).

151. F. Castelli, "Stimulated Emission of Cresyl Violet Pumped by N_2 Laser or Rhodamine 6G Dye Laser," Appl. Phys. Lett. 26(1), 18-19 (1975).

152. J. M. Telle and C. L. Tang, "New Method for Electro-Optical Tuning of Tunable Lasers," Appl. Phys. Lett. 24(2), 85-7 (1974).

153. F. Y. Wu, R. E. Grove, and S. Ezekiel, "CW Dye Laser for Ultrahigh-Resolution Spectroscopy," Appl. Phys. Lett. 25(1), 73-5 (1974).

154. T. W. Hansch, A. L. Schawlow, and P. Toschek, "Simple Dye Laser Repetitively Pumped by a Xenon Ion Laser," IEEE J. Quantum Electron. 9, 553-4 (1973).

155. S. J. Fielding, "An Intermediate-Laser-Dye-Laser System," J. Phys. E 7(4), 250-2 (1974).

156. I. Nagata and T. Nakaya, "Polarization of Dye Laser Light," J. Phys. D 6, 1870-92 (1973).

157. Y. Sugiura, Y. Matsunaga, and T. Fujioka, "Wavelength Measurements of Simultaneously Excited Superradiance and Laser Emission from Cryptocyanine Dye," J. Appl. Phys. 45(11), 4969-70 (1974).

158. B. Wellegehausen, H. Welling, and R. Beigang, "A Narrowband Jet Stream Dye Laser," Appl. Phys. 3, 387-91 (1974).

159. P. Burlamacchi, R. Pratesi, and R. Salimbeni, "High-Energy Planar Self-Guiding Dye Laser," Opt. Commun. 11(2), 109-11 (1974).

160. A. A. Zlenko, A. M. Prokhorov, and V. A. Sychugov, "Tunable Thin-Film Laser," Kvantovaya Elektron. (Moscow), No. 6(18), 74-8 (1973).

161. P. Burlamacchi and R. Pratesi, "High-Efficiency Coaxial Waveguide Dye Laser with Internal Excitation," Appl. Phys. Lett. 23(8), 475-6 (1973).

162. P. Burlamacchi and R. Pratesi, "Waveguide Dye Solution Lasers," Spectrosc. Lett. 8(9), 637-50 (1975).

163. G. Marowsky, "Gain-Narrowing Studies with an Organic Dye Laser," J. Appl. Phys. 45(6), 2621-3 (1974).

164 F. C. Strome, Jr., and J. P. Webb, "Flashtube-Pumped Dye Laser with Multiple Prism Tuning," Appl. Opt. 10(6), 1348-53 (1971).

165. G. Marowsky and F. Zaraga, "A Comparative Study of Dye Prism Ring Lasers," IEEE J. Quantum Electron. 10(11), 832-7 (1974).

166. G. Marowsky, "A Single-Mode Dye Ring Laser with Output Coupler Using Frustrated Total Internal Reflection," Z. Naturforsch., Teil A 29(3), 536-48 (1974).

167. M. Okada, S. Shimizu, and S. Ieri, "Tuning of a Dye Laser by a Birefringent Fabry-Perot Etalon," Appl. Opt. 14(4), 917-22 (1975).

168. W. Streifer and P. Saltz, "Transient Analysis of an Electronically Tunable Dye Laser--Part II: Analytic Study," IEEE J. Quantum Electron. 9(6), 563-9 (1973).

169. L. D. Hutcheson and R. S. Hughes, "Rapid Acousto-optic Tuning of a Dye Laser," Appl. Opt. 13(6), 1395-8 (1974).

170. L. Cirkovic and J. Jovicic, "Tuning of Dye Lasers by the Use of Christiansen Filters," Fizika 5 53-5 (1973).

171. P. B. Mumola, "Dye Laser Tuning with Pellicles," J. Appl. Phys. 44(7), 3198-9 (1973).

172. R L. Barger, M. S. Sorem, and J. L. Hall, "Frequency Stabilization of a CW Dye Laser," Appl. Phys. Lett. 22(11), 573-5 (1973).

173. W. Hartig and H. Walther, "High-Resolution Spectroscopy with and Frequency Stabilization of a cw Dye Laser," Appl. Phys. 1, 171-4 (1973).

174. H. Welling, H. W. Schroder, and B. Wellegehausen, "Frequency Stability and Linewidth of Single Mode CW Dye Lasers," Spectrosc. Lett. 8(9), 685-95 (1975).

175. T. R. Royt, W. L. Faust, L. S. Goldberg, and C. H. Lee, "Temporally Coincident Ultrashort Pulses from Synchronously Pumped Tunable Dye Lasers," Appl. Phys. Lett. 25(9), 514-16 (1974).

176. B. K. Garside and T. K. Lin, "Passive Mode-Locking in Flashlamp-Pumped Dye Lasers," Opt. Commun. 12(3), 240-5 (1974).

177. C. V. Shank and E. P. Ippen, "Subpicosecond Kilowatt Pulses from a Mode-Locked CW Dye Laser," Appl. Phys. Lett. 24(8), 373-5 (1974).

178. G. H. C. New, "Pulse Evolution in Mode-Locked Quasi-Continuous Lasers," IEEE J. Quantum Electron. 10(2), 115-24 (1974).

179. D. J. Bradley, "Generation and Measurement of Frequency-Tunable Picosecond Pulses from Dye Lasers," Opto-Electronics 6, 25-42 (1974).

180. A. E. Siegman and D. J. Kuizenga, "Active Mode-Coupling Phenomena in Pulsed and Continuous Lasers," Opto-Electronics 6, 43-66 (1974).

181. A. Dienes, "Mode-Locked CW Dye Lasers," Opto-Electronics 6, 99-113 (1974).

182. A. A. Friesem, U. Ganiel, and G. Neumann, "Simultaneous Multiple-Wavelength Operation of a Tunable Dye Laser," Appl. Phys. Lett. 23(5), 249-51 (1973).

183. J. M. Yarborough, "Multiple Dye Stream Laser," U.S. Patent 3,846,715 (November 1974); Chem. Abstr. 82, 37227y (1975).

184. J. S. Bakos, Z. Fuzessy, Zs. Sorlei and J. Szigeti, "Distributed Feedback Dye Laser of Wavelength Tunable from 7470 Å to 8400 Å," Phys. Lett. 50A(3), 227-8 (1974).

185. A. N. Rubinov and T. Sh. Efendiev, "Generation of Stimulated Radiation in a Dye Solution on Reflection from a Nonlinear Self-Induced Mirror," Kvantovaya Elektron. (Moscow), No. 3(15), 129-30 (1973).

186. L. S. Goldberg and J. M. Schnur, "Tunable Internal-Feedback Liquid Crystal-Dye Laser," U.S. Patent 3,771,065 (November 1973); Chem. Abstr. 80, 21324a (1974).

187. V. G. Ignat'ev and A. N. Tokareva, "The Influence of the Laser Pumping Cavity of the Characteristics of Pulsed Pumping Sources," Zh. Prikl. Spektrosk. 19(4), 632-5 (1973).

188. P. Dezauzier, A. Eranian, and O. deWitte, "Amplification Competition in a Double-Cavity Flash-Pumped Dye Laser," Appl. Phys. Lett. 22(12), 664-6 (1973).

189. J. C. Shah, "Laser with Means for Suppressing Background Fluorescence in the Output," U.S. Patent 3,739,295 (June 1973); Chem. Abstr. 79, 47754v (1973).

III. CHARACTERISTICS OF EXCIMER LASERS

General

A research program, largely sponsored by the Department of Defense, to investigate high-power high-efficiency gas lasers has developed a class of lasers that will find important applications in laser photochemistry. This class of lasers is based on excimers, i.e., atomic dimer aggregates which are unstable in their ground state but are stable when electronically excited.

The emission from an upper bound state to the dissociative ground state, which is characteristic of an excimer, is continuous over a range that is characteristic of the particular molecule. Excimer lasers can be tuned continuously over a portion of this continuous emission band, as has been demonstrated for several excimers. For example, in the xenon excimer--the subject of active research for several years--the fluorescent band has a width of $\sim$ 15 Å or one-third of the continuum width. A broader tuning range would be expected if cavity losses were reduced.

The characteristic emission spectra of rare-gas excimers have also been observed in other materials including rare gas-halides, halide excimers, and the vapors of metals with closed shells such as zinc, cadmium, and mercury.

The use of the term "excimer" has been commonly extended to describe dimer molecules that contain different monomer species and which would more properly be called exciplexes. In this discussion the term excimer loosely applies to excimers proper, to exciplexes, and to other metastable molecules with the characteristic emission of an excimer. Selected excimer lasers and promising species receiving attention are listed in Table VII, with reported tuning ranges, output energies, and conversion efficiencies representing the state of the art. As important as the high energies and high efficiencies that can be attained with these lasers, is their potential scalability to high energies and high pulse rates.

TABLE VII

HIGH-POWER UV LASERS

Laser	Wavelength (Å)	Tuning Range (Å)	Pulse Energy (J)	Efficiency (%)
XeF	3540	---	1	0.3-3
XeCl	3080	50	---	---
XeBr	2828	---	0.45	---
*XeI	2535	40	---	---
KrF	2480	70	100	3
			6	15-25
*KrBr	2030	---	---	---
ArF	1900	---	100	---
ArCl	1750	200	---	---
I_2	3430	---	1	---
*Cl_2	2600	800	---	---
*Br_2	2800	300	---	---
Ar-N_2	3577	---	0.2	1-3
*Xe-N_2	3130	200	---	---
*Hg_2	3350	500	---	---

Of the rare-gas halides, KrF (at 2480 Å) and XeF (at 3540 Å) lasers have produced the highest powers and efficiencies. Lasing has been achieved in both KrF and XeF under excitation with electron beams, with electron-beam-sustained electrical discharges, and with electrical discharges alone. In an electron-beam-pumped KrF laser, more than 100 J has been produced in a 55-ns pulse with a laser efficiency of 3.5%. The output of more recently developed discharge-pumped KrF lasers has been more modest, (≥ 100 mJ). Discharge-pumped lasers are of particular interest for photochemical applications becuase of their scalability to high pulse rates. Net efficiencies near 10% appear possible.

When successfully developed, these lasers will find applications in photochemistry, in laser-isotope separation, in pumping other lasers, and, possibly, in laser fusion. The molecular data and the knowledge of reaction kinetics acquired in this effort will lead to new pumping techniques for other laser systems. For example, the energy stored in rare-gas atoms and excimers can be transferred to other molecules or atoms through collisional transfer of excitation energy or through a photoprocess induced by the fluorescent emission of a rare-gas excimer.

Because this class of tunable lasers has been developed only very recently, it has not been mentioned in other reviews of potential uv potochemical light sources. The following discussion will provide a general background for evaluation of recent and future excimer laser developments.

Relevant Molecular Physics

In the excimer systems, the radiative emission of interest occurs in an electronic (or more precisely, a vibration-electronic) transition of a molecular complex. For such a transition, let (AC)* denote an upper energy state of the complex and (AC) the lower energy state, where A is an atom and C is either another atom or a molecule. The electronic state of (AC)* is one for which the molecular complex is not bound in most cases. If (AC) is the ground electronic state of the complex and is unbound, the potential surface for fragments A and C (1) is either repulsive (except for a small van der Waals minimum at large separations) or is too weakly attractive for binding, and (2) correlates at large separations with the fragments in their respective ground states. In some cases, (AC) has an excited electronic state that is repulsive and correlates with the atom A in its ground state and with the particle C either in its ground state or its first excited state. The other case of interest is that in which the molecular complex (AC) is weakly bound. The rare-gas monohalide XeF (which combines the heavy noble gas xenon with the lightest halogen fluorine) appears to be weakly bound in the ground electronic state, with a potential-energy well deep

enough to support some few vibrational levels. There is evidence that XeCl in the ground electronic state is also bound.

The bound complex (AC)* is called an exciplex (excited complex) when C is a molecule, and is called an excimer (excited dimer) when A and C are atoms of the same kind. Generally, the term excimer has been extended to the case of a diatomic molecule whose atoms A and C are different.

Typical, potential-energy curves for various excimer systems are shown in Fig. 7. Many homonuclear diatomic excimers A_2^*, as typified by the argon dimer shown in Fig. 7a, are bound by covalent bonding forces. For the rare-gas excimers, the two lowest bound electronic states are the lowest-lying triplet $^3\Sigma_u^+$ and excited singlet $^1\Sigma_u^+$ configurations of the molecule.[1] At large separations, these states correlate respectively with one atom in the metastable $^3P_2$ or the $^3P_1$ level of the first atomic doublet term and with the other atom in the $^1S_0$ ground term. The singlet-triplet splitting is due to spin-orbit coupling, and is relatively small for argon. For a heavier rare-gas excimer, these bound singlet-triplet states lie lower relative to the ground-state potential but have a larger splitting. The ground-state potential-energy curve relates to two closed-shell atoms and is repulsive. Radiative transitions occur from the discrete vibrational levels (or, more precisely, from the rotational sublevels of the vibrational levels) of an excited electronic state to the unbound ground state. According to the Franck-Condon principle, transitions from a vibrational level take place (1) only to a spread of points on the lower potential curve corresponding to internuclear separations accessible to the initial vibrational motion, and (2) with transition intensity proportional to the square of the overlap integral between the initial and final wave functions of nuclear motion. Because the potential energy (for nuclear motion) in the lower electronic state lies on a continuous dissociative curve, the spectrum is continuous and has a frequency width proportional to the slope of the repulsive potential curve. The spontaneous emission from such bound-free transitions is a

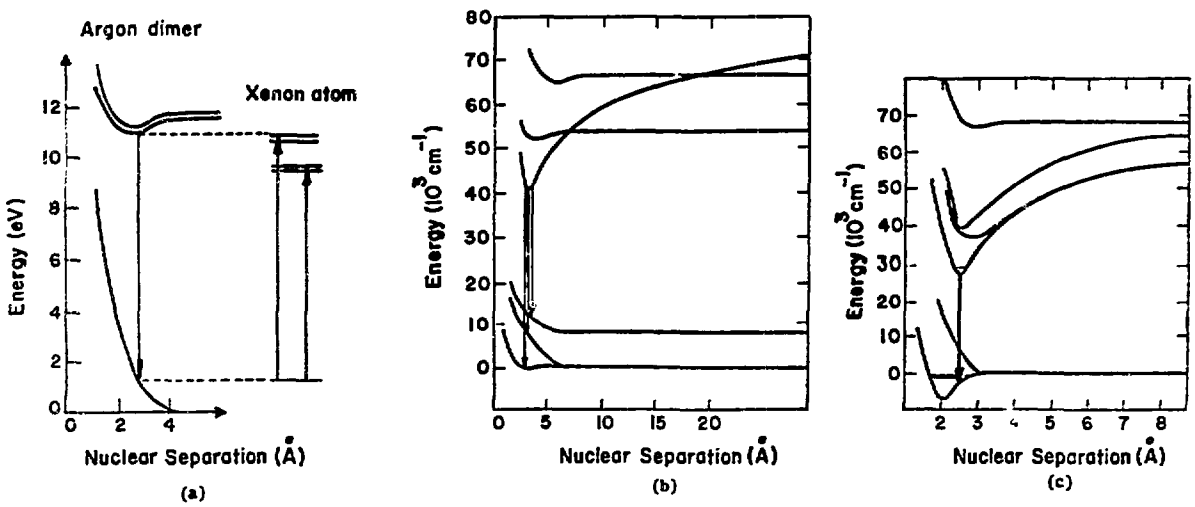

Fig. 7. Potential energy curves for (a) argon dimer and xenon atom showing resonant transfer, (b) xenon iodide, and (c) xenon fluoride. For simplicity only the lowest-lying excited states are shown.

continuum band centered approximately at the emission center of the lowest vibrational level (~ 1300 Å in the case of the argon dimer). The band width includes the energy spread of the occupied vibrational levels (~ 2 kT) plus the width attributable to the slope of the lower-state potential. The excimer spontaneous emission for the rare gases typically has a 10% band width ($\Delta\nu_{sp} \sim 0.1\ \nu_o$). For a list of experimental studies of continuum emission by the rare gases in the vacuum ultraviolet see Ref. 2.

Excimer systems similar to the rare-gas excimers occur for the closed-shell metal atoms zinc, cadmium, and mercury, the best known being that of mercury.[3] The first and second excited state of the mercury dimer ($^3O_u^-$ and $^3\Pi_u$, respectively) are bound, while the ground state ($^1\Sigma_g^+$) is repulsive. Bound-free transitions from the excimer states to the molecular ground state produce broad continuum bands centered at 4570 and 3500 Å. These bands have usually been identified with mercury excimer transitions to the ground state, but the spectroscopic assignments are not firmly established.[4]

The excimer states of homonuclear diatomic molecules with repulsive ground states are formed mainly by associative combination of a metastable atom A* with a ground-state atom A in a three-body collision,

$$A^* + A + M \rightarrow A_2^* + M \ , \qquad (1)$$

where M is a third heavy particle.

Emission continua due to bound-free transitions are also observed for homonuclear diatomic molecules whose ground electronic state $^1\Sigma_g^+$ is tightly bound. In such cases a continuum spectrum corresponds to transitions from a bound triplet electronic state to a lower repulsive triplet state arising from two ground-state atoms. Even though the ground state and the repulsive triplet state both correlate at large separations to two normal atoms, radiative transition to the triplet is favored from a bound triplet state. The continuous spectrum of the hydrogen molecule, which extends from 1600 to 5000 Å, is a well-known example.[3] This spectrum contains contributions from vibrational levels of the lowest bound triplet state $^3\Sigma_g^+$ to the repulsive state $^3\Sigma_u^+$ resulting from two ground-state atoms. The great width of the continuum emission is caused by the steep potential curve in the lower state and by the number of contributing vibrational levels in the upper state.

Certain physical and chemical properties of the metastable states of the heavy rare-gas atoms which arise from the first excited configuration $np^5(n+1)s^1$ are similar to the corresponding states of the nearest alkali atom in the periodic table. The excited states of a rare-gas monohalide are closely analogous to the nearest alkali halide both in binding energy and in gross structural properties.[5-7] Examples are shown in Fig. 7b for XeI and in Fig. 7c for XeF. The lowest states of the rare-gas halides are van-der-Waals and, in some cases, covalent bonded. The ground-term doublet $^2P_{3/2}$, $^2P_{1/2}$ of the halogen atom, which has a much larger splitting in iodine than in fluorine, forms upon approaching the ground-state noble-gas atom the states $^2\Sigma_{1/2}$, $^2\Pi_{3/2}$, $^2\Pi_{1/2}$, where $^2\Sigma_{1/2}$ is the ground molecular state. The deeply bound excited states of a rare-gas monohalide RX, where X is the halogen atom, are predominantly ionic with the polarity R^+X^-. The ionic excited states have the symmetry species $^2\Sigma_{1/2}$, $^2\Pi_{3/2}$, or $^2\Pi_{1/2}$, and are shown in Fig. 7c with the same ordering as the lower states (on the assumption that similar molecular orbital arguments apply). The ground state of XeI is only weakly attractive (possibly only van der Waals attraction), but the attractive well depth and covalent character probably increase in the sequence XeI, XeBr, XeCl, XeF due to

the greater electronegativity of the lighter halides. The lowest II states are always repulsive.

The $^2\Sigma^+_{1/2} \rightarrow {}^2\Sigma^+_{1/2}$ emission band for XeI and for XeBr is asymmetric, with a fairly sharp peak at the red edge (corresponding to the lowest vibrational level of the ionic upper state), and is shading off into the blue with a diffuse vibrational structure superimposed on the continuum (corresponding to emission from various vibrational states of the ionic upper state). In XeI, the emission band edge is at ~ 2549 Å and ~ 95% of the emission is found between 2510 and 2549 Å. The narrowness of the band indicates that the lower-state potential curve for this bound-free transition is not changing rapidly with internuclear separation in the neighborhood of the transition. The corresponding band for XeBr is much wider. The $^2\Sigma^+_{1/2} \rightarrow {}^2II_{3/2}$ (3250 Å) band and the $^2\Sigma_{1/2} \rightarrow {}^2II_{1/2}$ (3600 Å) band of XeI are broad and fairly symmetric, indicating strongly repulsive lower-state potentials.

The $^2\Sigma \rightarrow {}^2\Sigma$ band of the XeF molecule peaks near 3530 A and shades off to the blue, with a general shape similar to that of the corresponding bands of the other xenon halides. However, much more structure appears with spacings smaller than the vibrational spacing of the upper ionic state. This is expected if the $^2\Sigma \rightarrow {}^2\Sigma$ transition in this species is bound-bound and terminates on bound vibrational levels of the lower-state potential well. The chemical binding of the upper and lower states differs (ionic and covalent, respectively), and the potential minima of the two curves are therefore expected to occur at different internuclear separations, with the upper state having the larger separation. Hence, the vertical transitions required by the Franck-Condon principle terminate on vibrational levels located near the top of the lower-state potential well.

Continuous emission bands have long been known for I_2 and Br_2.[2,8-10] Recently, laser action has been obtained on the strong I_2 band whose broad spectrum extends from 3000 to 3450 Å.[11-13] The electronic states responsible for this band have not yet been identified. It appears that the upper electronic state of this I_2 transition is a bound ionic state (the $^3II_{2g}$ or $D^1\Sigma^+_u$), which correlates to the separated ion pair $I^+ + I^-$, whereas the lower state is one of the covalent states (the unbound $^3II_{2u}$ or the bound $X^1\Sigma^+_g$ ground state, respectively) that correlates to two ground-state iodine atoms. Wideband emission of Br_2 peaked at 2920 Å, as just reported, appears by comparison to I_2 to be significantly less efficient with evidence that output energy is severely limited by lower-level bottlenecking.

The ionic excited states of the rare-gas monohalides can be formed by various kinds of reactions. The halogen molecule X_2 or other halogen donor compound CX (where C denotes the other molecular constituents) can react chemically with an electronically excited rare-gas atom R* to produce the excimer state (RX)*,

$$R^* + X_2 \rightarrow (RS)^* + X;$$

$$R^* + CX \rightarrow (RX)^* + C, \qquad (2)$$

with a large reactive cross section. The ionic excited state (RX)* can also be formed by rapid (at high pressures) three-body Thompson recombination of X^- ions with R^+ ions:

$$R^+ + X^- + M \rightarrow (RX)^* + M; \qquad (3a)$$

or by excimer exchange:

$$(R'X)^* + R \rightarrow (RX)^* + R', \qquad (3b)$$

where R' is a different rare-gas species in the mixture. Three-body ion recombination appears to be the dominant production mechanism of the I_2 excimer:

$$I^- + I^+ + M \rightarrow I_2^* + M;$$

$$I^- + CI^+ + M \rightarrow I_2^* + C + M \ . \qquad (4)$$

In general, the excimers are also formed in a state of vibrational excitation, but at higher pressures vibrational relaxation to lower vibrational levels proceeds rapidly by two-body collisions with the heavy particles in the gas.

The rare gas-monohalide formation reactions, Eq. (2), are the only known exothermic bimolecular chemical reactions that give electronically excited products with visible or uv emission. The large cross sections and favorable branching ratios of these reactions (comparable to the analogous alkali-plus-halogen reactions) contribute to the high potential laser efficiency of these systems. Moreover, excimer formation processes involving two-body collisions can have rapid kinetic rates at lower pressures than the molecular formation processes indicated by Eq. (1) and hence are more suitable for electric discharge excitation.

Oxygen atoms in the metastable $O(^1S_o)$ excited level in three-body collisions involving a ground-state rare-gas atom $R(^1S_o)$ can form the rare gas-oxygen excimer $RO(2^1\Sigma^+)$, which correlates at large nuclear separations to $R(^1S_o) + O(^1S_o)$, where R is xenon, krypton, or argon. The most tightly bound of these is the $XeO(2^1\Sigma^+)$[14,15] excimer, which still has a relatively shallow potential well (~ 0.06 eV). Various spontaneous emissions occur from the $2^1\Sigma^+$ state. The green-band emissions are bound-bound transitions to two lower excimer states, the more tightly bound (~ 0.34-eV) $1^1\Sigma^+$ and the very weakly bound (~ 0.025-eV) $1^1\Pi$ state, both of which correlate to $Xe(^1S_o) + O(^1D_2)$. The generally used band assignment for the major green bands (4800 to 5600 Å) is $2^1\Sigma^+ \rightarrow 1^1\Sigma^+$, and for the minor green bands (5600 to 5800 Å) is $2^1\Sigma^+ \rightarrow 1^1\Pi$. Another emission is a uv continuum band (centered at ~ 3080 Å) to a repulsive lower state, probably $1^3\Pi$, which correlates to both xenon and oxygen atoms in their ground terms. These emission bands correlate with the various dipole forbidden transitions in the oxygen atom, namely the auroral green line at 5577 Å between the oxygen metastable states $O(^1S_o) \rightarrow O(^1D_2)$ and the transauroral line at 2972 Å between $O(^1S_o) \rightarrow O(^3P_1)$. The emission bands of the rare gas-oxygen excimers may be interpreted as shifted, broadened, and intensified (induced dipole) forms of the pure atomic lines, resulting from the perturbing effect of the molecular binding. The green and uv bands of the XeO excimer holds promise of efficient laser operation.[16,17]

Excimer emission from ArH has been observed,[18,19] as well as the emission continua from excimers of HgXe, $Hg(H_2O)$, and $Hg(NH_3)$.[20-23] Laser systems based on continuum emissions from excimers of alkali-rare gas diatomics and from excited alkali dimers have been predicted.[24,25] Recently, strong $\Sigma \rightarrow X\Sigma$ emission bands of the cesium-rare gas excimers have been observed, with prominent peaks at 5615 Å (CsAr), 5650 Å (CsKr), and 5725 Å (CsXe) and widths of ~ 50 Å. Similar emissions occur from the rubidium-rare gas excimers.[26,27] The alkali-rare gas molecules of the lighter alkalis sodium and potassium are expected to have stronger binding in the excimer state and greater repulsion in the ground state.[28] The observed emission spectra from the latter excimers confirm that the corresponding bands are broader and more red-shifted from the forbidden 4s → 3s transition of the relevant alkali atom.[28] Efforts to attain lasing in an alkali-rare gas system are in progress.[29]

Another recently observed emission band extending from 2200 to 3000 Å has been assigned to a bound-free transition of the Cl_2 molecule and shows promise for an efficient tunable laser in the uv.[30] Gas-phase emission bands of interest for laser applications are listed in Table VIII.

TABLE VIII

EXCIMER EMISSIONS

Molecular Species	Fluorescent Emission Peak (Å) [FWHM]	Observed Laser Emission Wavelength (Å)
Xe_2	1720 [150]	1720
Kr_2	1460 [140]	1457
Ar_2	1260 [80]	1261
Hg_2	4850 [1300]	---
	3350 [600]	---
XeF	4500	---
	3530 [25]	3532,3511
	2650 [15]	---
XeCl	4250	---
	3080 [23]	3081,3079
XeBr	4650	---
	3530	---
	2820 [34]	2828
XeI	3600 [540]	---
	3250 [160]	---
	2540 [20]	---
KrF	3050	---
	2486 [20]	2484,2491
ArF	1933 [40]	1933
I_2	3420 [50]	3425,3424, 3420,3420
	2870 [20]	---
XeO	5680 [35]	---
	5450 [140]	5530,5470, 5390
KrO	5578 [25]	5578
ArH	7670	---
NaAr	4239 [185]	---
NaKr	4299 [220]	---
NaXe	4407 [220]	---
KAr	5082 [200]	---
KKr	5119 [245]	---
KXe	5205 [260]	---
RbAr	4960 [20]	---
RbKr	5000 [20]	---
RbXe	5017 [20]	---
CsAr	5616 [45]	---
CsKr	5648 [45]	---
CsXe	5723 [60]	---
HgXe	2700 [150]	---
$Hg(H_2O)$	2890 [250]	---
$Hg(NH_3)$	3500 [400]	---

Laser Action on Excimer Transitions

Laser action has now been demonstrated on many excimer transitions. Lasing can occur when the excimers are produced in sufficient density within an optical cavity. In the first demonstration experiments, mirrors at each end of an excitation cell have provided sufficient feedback for the buildup of amplified spontaneous emission. Pulsed lasing occurs at one or more oscillation frequencies, which are generally near peaks in the fluorescent emission band. Early experiments led to only limited optimization of optical cavities, molecular mixtures, and operating conditions for maximum efficiency. Thus, present efficiencies are in most cases well below attainable values. Earliest developments in excimer lasers are discussed in various reviews.[31-34]

Laser action is characterized by the simultaneous occurrence of (1) spectral line narrowing, (2) spatial coherence of the directed output beam, (3) a sharp oscillation threshold for the onset of laser emission, (4) a time dependence of the radiation pulse (onset time and narrowed pulse duration) that differs markedly from that of the spontaneous emission, and (5) a large increase in axial light intensity within the optical cavity (accompanied by a dip in spontaneous emission when the laser emission is relatively strong).

When the lower state is unbound, the spread of Franck-Condon vertical transitions from the bound upper state corresponds to a range of positions on the dissociative lower potential curve and hence to a range of final energies for the molecular complex. The energy range increases directly with the slope of the dissociation curve in the neighborhood of the transition. Thus, a bound-free transition gives a continuous emission band and has the potential of continuously tunable laser operation over a part of the band.

Tunability has been demonstrated in the case of the xenon excimer transition,

whose lower state is the repulsive ground state of Xe_2.[35] The fluorescent band is centered at 1720 A with a width ~150 Å. A prism acting as a dispersive element in the optical cavity enabled the laser emission to be tuned over a range of 50 Å (1700 cm^{-1}) around the central wavelength. The tuning range would increase to a higher fraction of the continuum width (150 A) if cavity losses could be reduced. Similar tuning ranges are expected for the krypton and argon lasers. In the case of an emission spectrum that shows considerable structure due to closely spaced vibrational bands, such as the bound-bound transitions of XeF centered at 3540 Å or the mixed-type transitions of I_2 at 3420 Å, the laser emission presumably could be discretely tuned over the series of peaks.

Lasers based on an excimer transition to an unbound state are called molecular dissociation lasers, because the molecular complex dissociates after emission,

$$(AC)^* \rightarrow (AC) + h\nu \ , \qquad (5a)$$

$$(AC) \rightarrow A + C \ . \qquad (5b)$$

The molecule in the lower electronic state disintegrates in a time comparable to one vibrational period (10^{-13} s). The position of (AC) on the dissociation curve following the transition (namely, the height above the separation asymptote) determines the kinetic energy of fragments A and C after separation.

When the unbound lower state is the ground electronic state, the inverse process to that of Eqs. (5a) and (5b) must also be considered. Ground-state particles A and C in a binary collision approach along the ground-state repulsive potential curve of A+C and are said to be in the state of collision (state of the quasi-molecule).[3] If the internuclear separation on the lower potential curve reaches the region corresponding to the radiative emission from (AC)*, then absorption of a photon $h\nu$ at that position in the state of collision causes a vertical transition to the bound excimer state (AC)*. Thus, some fraction of the quasi-molecules formed during thermal collisions can absorb the photons emitted by the excimers and constitutes an effective lower-state population. At high pressures, the collision frequency is large and the density of quasi-molecules having large Franck-Condon factors with the excimer state (AC)* could be quite large. However, if the radiative transitions terminate at points on the lower curve at a distance appreciably greater than kT above the separation asymptote, the thermal population in the lower state will be small. Furthermore, the dissociation of the excimer molecule following stimulated emission is rapid on the time scale of laser pulses, 10^{-10} s or longer. Under these conditions, ground-state absorption is negligible, and the population inversion for the lasing transition is equal to the number of excimer molecules. Thus, under these conditions, bound-free excimer transitions have the advantage that all the energy (above the threshold inversion) deposited in the excimer molecules can be extracted as photon energy.

Even in the case of bound-bound excimer transitions, the conditions for population inversion are generally favorable. The upper and lower potential curves are usually displaced, with the minimum of the upper curve at a larger internuclear separation. Vertical transitions from lower vibrational levels of the upper potential will terminate on higher vibrational levels of the lower potential. Thermal occupation of the latter levels is small, and fast vibrational relaxation at high pressures will empty them rapidly and thus prevent bottlenecking in the lower laser level.

The primary consideration in evaluating a particular excimer transition for laser application is the relative probability for photoabsorption and stimulated

emission from the excimer state. Many excimers have either (1) higher electronic states (bound or repulsive) of the complex, or (2) a photoionization or photodissociation continuum that can be reached from the excimer state by absorption of a laser photon. During laser action, photoabsorption from the excimer state $(AC)^*$ competes directly with stimulated emission to the lower state, and the net gain coefficient is directly proportional to the difference between their cross sections. Of course, photoabsorption by rare-gas metastable atoms or by other species (including impurities) in the mixture will reduce the gain as well as the efficiency.

Excimer state photoionization certainly occurs in the rare-gas excimers. The rare-gas molecules have an electronic energy-level structure similar to that of the rare-gas atoms. The first excited levels $^3\Sigma_u^+$ or $^1\Sigma_u^+$ lie high above the ground state $^1\Sigma_g^+$, followed by a relatively narrow series of Rydberg levels (energy levels of an electron in the field of the bound ion core R_2^+) to the first ionization limit. Hence the photon energy from a $\Sigma_u^+ \rightarrow \Sigma_g^+$ transition is sufficient to photoionize the Σ_u^+ state. The efficiency in laser emission (defined as fraction of electron-beam energy deposited in the gas that is converted to laser optical output energy) obtained with the rare-gas excimers has been somewhat disappointing (~ 1%) in view of their good fluorescence efficiency (defined as ratio of excimer fluorescent energy output to e-beam energy deposited in the gas) of ~ 6 to 25%. Excimer photoionization accounts for much of the lowered efficiency. Over much of the visible (4850 Å) band of the mercury dimer (or possibly trimer), which has generally been assigned to transitions from the $^3O_u^-$ excimer state to the ground state, the photoabsorption cross section in the upper state appears to exceed the stimulated-emission cross section resulting in negative gain.[4,36-38] Thus, laser action on this band can occur, if at all, only at selected regions of the band and probably with low efficiency. However, efficient laser action on the uv (3350 Å) band appears highly promising. In the hydrogen molecule photoionization from the lowest bound triplet state $a^3\Sigma_g^+$ appears to overwhelm the stimulated-emission gain throughout the 1600-to-5000-Å continuum.[39]

The first excited state R^* of the rare-gas atom R lies high above the ground level, but the level structure above R^* and the low ionization energy for R^* are similar to the excited level structure of the alkali atom A nearest to R in the periodic table. The excited electronic states of the rare-gas monohalide RX are mainly ionic, and the ion pair R^+X^- is analogous to the alkali halide A^+X^-. For a heavy rare gas R, the first excimer state of RX lies considerably lower than that of R_2, and photoionization by excimer emission is either eliminated or substantially reduced, which contributes greatly to the higher efficiency of many rare-gas monohalide lasers. Also, the rare-gas monohalides emit in the near-uv, where the optical problems (particularly at high beam flux) are much less severe than those in the vacuum-uv.

An excimer state decays either by spontaneous emission or by collisional deactivation. In the dense media of interest, excimer state lifetimes are generally less than 100 ns. For a rare-gas dimer, the fully allowed radiative decay of the singlet excimer has a lifetime of ~ 5 ns, whereas the triplet excimer is considerably longer lived, e.g., ~ 100 ns for xenon and ~ 2 μs for argon. At high gas pressure, continual mixing of singlet and triplet states occurs by excimer collisions with atoms and secondary electrons. The excimer states of the rare-gas monohalides have radiative lifetimes of the order of 50 ns. In the case of the rare gases, excimer-excimer annihilation by Penning ionization

$$R_2^* + R_2^* \rightarrow R_2^+ + R + R + e \qquad (6)$$

is the dominant collisional deactivation process at high excimer densities. For rare gas monohalides and I_2, kinetic deactivation of the excited state occurs mainly by two-body collisional quenching to the ground state by ground-state rare gas atoms or by molecular species in the mixture:

$$(RX)^* + M \rightarrow (RX) + M \; . \qquad (7)$$

Because the energy separation between the excimer and ground state is large at all internuclear distances, the rate constant for rare-gas excimer quenching to the ground state by superelastic collisions with ground-state atoms is expected to be small compared to excimer quenching by Process (6). But, in the case of rare-gas-monohalides, excimer quenching by ground-state atoms appears to be large for krypton and xenon. Also, quenching by halogen donor molecules M with bond rupture of M can be large.

We mention that the primary collisional loss mechanism of rare-gas metastable atoms at high densities is the atomic analogue of Process (6), namely, mutual annihilation of metastables by Penning ionization:

$$R^* + R^* \rightarrow R^+ + R + e \; . \qquad (8)$$

Rare-gas metastable atoms and excimer molecules are also lost through excitation or ionization by relatively low-energy electrons (≥ 3.8 eV for ionization of xenon metastables). The electron-impact ionization cross section of R* by low-energy electrons is generally large compared to the electron cross section for excitation of the ground state R. Under the high electron-density conditions of laser pumping, deactivation by electron collisions is expected to be important.

The total line strength of an excimer emission, although large, is spread in the case of a bound-free transition over a continuum with a large bandwidth ($\Delta\nu \sim 100$ Å). Accordingly, stimulated-emission cross sections for bound-free transitions are several orders of magnitude smaller than comparable bound-bound transitions. Stimulated-emission cross sections (at line center) for continuum transitions, σ_{SE}, are typically in the range 10^{-19} to 10^{-18} cm^2, whereas for XeF, where the $^2\Sigma \rightarrow {}^2\Sigma$ transitions are discrete, $\sigma_{SE} \approx 2 \times 10^{-16}$ cm^2.

In view of practical limitations on laser pumping rates, the mean lifetime of the upper lasing level (for spontaneous emission and nonradiative decay processes) limits the attainable inversion density in the medium. Hence, the short decay lifetime of excimer states restricts the energy-storage capability in these systems. Because the cross section for stimulated emission associated with a wide continuum band is small, excimer density must be high for adequate small-signal gain. But to obtain large excimer densities with short excimer lifetimes, a high-density lasing medium is required. Hence, sufficient gain for laser operation generally requires a high-pressure gas or a liquid. In such high-pressure media, collision processes are generally fast compared to spontaneous radiative processes, including the three-body collision processes required for rare-gas excimer formation. A small cross section for stimulated emission with a short upper-level quenching time implies a large pumping-power density to produce the threshold-inversion density for initiating laser action on the transition. The extremely high pumping-power density required for the low-gain dissociation lasers will probably limit their operation to short (40 to 100 ns) pulsed excitation of dense media. On the other hand, quasi-cw operation is possible for the higher-gain lasers, particularly those based on bound-bound transitions (such as XeF and I_2), provided

bottlenecking does not occur at the lower level.

Operating densities are limited by the rate of collisional loss processes (6) or (7) and (8), which deplete the excitation energy stored in the excimers and rare-gas metastables. Moreover, in a rare gas-monohalide laser, the desired excimer formation , Process (2), must compete with termolecular rare-gas dimerization, Process (1), which is a loss process in the kinetics and becomes increasingly important at high partial pressures of the rare gas. Formation of rare-gas excimers reduces the efficiency of converting energy deposited in the gas into laser emission, and may even block laser emission at high pressures if the rare-gas excimer absorbs photons at the laser frequency. Photoabsorption by the xenon excimer formed in the Xe-Br_2 mixture probably accounts for the blockage of the XeBr excimer laser that occurs at pressures above ~ 1 atm.

From the lowest pressure at which laser action occurs, total laser emission has generally been observed to increase linearly with pressure over some range of pressures (under conditions of e-beam excitation where the energy deposition per unit volume is very nearly proportional to the density of the gas mixture). In this range, laser efficiency increases with pressure because of favorable rate increases of desired energy transfers in the kinetic chain. As the pressure increases beyond the region of linear output, the rate of the collisional deactivation processes (6) or (7) and (8) will have increased sufficiently to cause laser efficiency to decrease. With relatively small additional pressure rise, total laser emission begins to fall off as collisional decay of the excimer dominates the kinetics. In the rare-gas excimers laser emission at elevated gas densities decreases further as a result of the mixing between the relatively close $^3\Sigma_u$ and $^1\Sigma_u$ excimer states by collisions with low-energy electrons (rate $\propto p^{1/2}$ tending to equalize the populations) and with heavy particles (rate $\propto p$ favoring electronic relaxation to the triplet level). The small stimulated-emission cross section for the partially forbidden transition from the triplet level may even be exceeded by the photoionization cross section. At very high pressures where heavy particle collisions dominate, the shift of populations to the triplet state lowers both the optical gain and the laser emission.

Laser emission generally peaks near the pressure and mixture with the greatest fluorescent emission. In the case of the rare-gas excimers under e-beam excitation, optimum pressure for the xenon laser[2,40-45] is about 15 atm in pure xenon (and about the same partial pressure of xenon in Xe-Ar mixtures), for the krypton laser[43] about 30 atm, and for argon[46] about 55 atm. The molecular xenon laser has the highest output power and efficiency. Approximately the same respective pressures of xenon and krypton (with 5 to 10 torr of O_2) give optimum performance of the XeO and KrO lasers.[16] Gain in the ArO system has only recently been reported for mixtures with up to 40 atmospheres of argon and a few torr of N_2O.[47] At high pressures ($\geq$ 10 atm) the discrete rotational-vibrational lines broaden and overlap into continuous emission bands. For the rare gas-monohalides[48-57] and iodine[11-13] lasers under e-beam excitation, optimum total pressure of the gas mixtures are considerably less (~ 2 to 5 atm), e.g., output of the KrF laser[50,54,55] peaks at 3 to 4 atm and of XeF[51,52,56] at about 1.5 to 2.5 atm.

In the rare-gas excimer lasers, photoabsorption by ground-state quasi-molecules (formed during collisions of ground-state atoms in thermal motion) not only increases with density, but also increases rapidly with temperature rise of the gas mixture. Ground-state absorption lowers the extractable part of the deposited energy density and thereby degrades laser performance. It has been demonstrated in the xenon laser[44]

$$R_2^* + R_2^* \rightarrow R_2^+ + R + R + e \qquad (6)$$

is the dominant collisional deactivation process at high excimer densities. For rare gas monohalides and I_2, kinetic deactivation of the excited state occurs mainly by two-body collisional quenching to the ground state by ground-state rare gas atoms or by molecular species in the mixture

$$(RX)^* + M \rightarrow (RX) + M \ . \qquad (7)$$

Because the energy separation between the excimer and ground state is large at all internuclear distances, the rate constant for rare-gas excimer quenching to the ground state by superelastic collisions with ground-state atoms is expected to be small compared to excimer quenching by Process (6). But, in the case of rare-gas-monohalides, excimer quenching by ground-state atoms appears to be large for krypton and xenon. Also, quenching by halogen donor molecules M with bond rupture of M can be large.

We mention that the primary collisional loss mechanism of rare-gas metastable atoms at high densities is the atomic analogue of Process (6), namely, mutual annihilation of metastables by Penning ionization

$$R^* + R^* \rightarrow R^+ + R + e \ . \qquad (8)$$

Rare-gas metastable atoms and excimer molecules are also lost through excitation or ionization by relatively low-energy electrons ($\geq$ 3.8 eV for ionization of xenon metastables). The electron-impact ionization cross section of R^* by low-energy electrons is generally large compared to the electron cross section for excitation of the ground state R. Under the high electron-density conditions of laser pumping, deactivation by electron collisions is expected to be important.

The total line strength of an excimer emission, although large, is spread in the case of a bound-free transition over a continuum with a large bandwidth ($\Delta\nu$ ~ 100 Å). Accordingly, stimulated-emission cross sections for bound-free transitions are several orders of magnitude smaller than comparable bound-bound transitions. Stimulated-emission cross sections (at line center) for continuum transitions, σ_{SE}, are typically in the range 10^{-19} to 10^{-18} cm^2, whereas for XeF, where the $^2\Sigma \rightarrow {}^2\Sigma$ transitions are discrete, $\sigma_{SE} \sim 2 \times 10^{-16}$ cm^2.

In view of practical limitations on laser pumping rates, the mean lifetime of the upper lasing level (for spontaneous emission and nonradiative decay processes) limits the attainable inversion density in the medium. Hence, the short decay lifetime of excimer states restricts the energy-storage capability in these systems. Because the cross section for stimulated emission associated with a wide continuum band is small, excimer density must be high for adequate small-signal gain. But to obtain large excimer densities with short excimer lifetimes, a high-density lasing medium is required. Hence, sufficient gain for laser operation generally requires a high-pressure gas or a liquid. In such high-pressure media, collision processes are generally fast compared to spontaneous radiative processes, including the three-body collision processes required for rare-gas excimer formation. A small cross section for stimulated emission with a short upper-level quenching time implies a large pumping-power density to produce the threshold-inversion density for initiating laser action on the transition. The extremely high pumping-power density required for the low-gain dissociation lasers will probably limit their operation to short (40 to 100 ns) pulsed excitation of dense media. On the other hand, quasi-cw operation is possible for the higher-gain lasers, particularly those based on bound-bound transitions (such as XeF and I_2), provided

bottlenecking does not occur at the lower level.

Operating densities are limited by the rate of collisional loss processes (6) or (7) and (8), which deplete the excitation energy stored in the excimers and rare-gas metastables. Moreover, in a rare gas-monohalide laser, the desired excimer formation , Process (2), must compete with termolecular rare-gas dimerization, Process (1), which is a loss process in the kinetics and becomes increasingly important at high partial pressures of the rare gas. Formation of rare-gas excimers reduces the efficiency of converting energy deposited in the gas into laser emission, and may even block laser emission at high pressures if the rare-gas excimer absorbs photons at the laser frequency. Photoabsorption by the xenon excimer formed in the $Xe-Br_2$ mixture probably accounts for the blockage of the XeBr excimer laser that occurs at pressures above ~ 1 atm.

From the lowest pressure at which laser action occurs, total laser emission has generally been observed to increase linearly with pressure over some range of pressures (under conditions of e-beam excitation where the energy deposition per unit volume is very nearly proportional to the density of the gas mixture). In this range, laser efficiency increases with pressure because of favorable rate increases of desired energy transfers in the kinetic chain. As the pressure increases beyond the region of linear output, the rate of the collisional deactivation processes (6) or (7) and (8) will have increased sufficiently to cause laser efficiency to decrease. With relatively small additional pressure rise, total laser emission begins to fall off as collisional decay of the excimer dominates the kinetics. In the rare-gas excimers laser emission at elevated gas densities decreases further as a result of the mixing between the relatively close $^3\Sigma_u$ and $^1\Sigma_u$ excimer states by collisions with low-energy electrons (rate $\propto p^{1/2}$ tending to equalize the populations) and with heavy particles (rate $\propto p$ favoring electronic relaxation to the triplet level). The small stimulated-emission cross section for the partially forbidden transition from the triplet level may even be exceeded by the photoionization cross section. At very high pressures where heavy particle collisions dominate, the shift of populations to the triplet state lowers both the optical gain and the laser emission.

Laser emission generally peaks near the pressure and mixture with the greatest fluorescent emission. In the case of the rare-gas excimers under e-beam excitation, optimum pressure for the xenon laser[2,40-45] is about 15 atm in pure xenon (and about the same partial pressure of xenon in Xe-Ar mixtures), for the krypton laser[43] about 30 atm, and for argon[46] about 55 atm. The molecular xenon laser has the highest output power and efficiency. Approximately the same respective pressures of xenon and krypton (with 5 to 10 torr of O_2) give optimum performance of the XeO and KrO lasers.[16] Gain in the ArO system has only recently been reported for mixtures with up to 40 atmospheres of argon and a few torr of N_2O.[47] At high pressures ($\gtrsim$ 10 atm) the discrete rotational-vibrational lines broaden and overlap into continuous emission bands. For the rare gas-monohalides[48-57] and iodine[11-13] lasers under e-beam excitation, optimum total pressure of the gas mixtures are considerably less (~ 2 to 5 atm), e.g., output of the KrF laser[50,54,55] peaks at 3 to 4 atm and of XeF[51,52,56] at about 1.5 to 2.5 atm.

In the rare-gas excimer lasers, photoabsorption by ground-state quasi-molecules (formed during collisions of ground-state atoms in thermal motion) not only increases with density, but also increases rapidly with temperature rise of the gas mixture. Ground-state absorption lowers the extractable part of the deposited energy density and thereby degrades laser performance. It has been demonstrated in the xenon laser[44]

provides an efficient process for the generation of xenon metastables. This makes it possible to operate the xenon laser at low densities of xenon atoms just sufficient for rapid formation of the xenon excimer by process (1). The argon diluent also reduces the temperature rise in the gas during e-beam irradiation. The lower density of xenon atoms and smaller temperature rise eliminate the detrimental effects of ground-state absorption and increase the output intensity of the xenon laser.

More generally, the energy residing in e-beam-excited, dense, rare gases can excite by energy-transfer collisions an additive species of atom or molecule in the gas, producing thereby an inversion on an electronic transition of the additive species. Energy-transfer pumping of the second positive band ($C^3\Pi_u \rightarrow B^3\Pi_g$) nitrogen laser has been demonstrated for Ar-N_2 mixtures.[4,60,64,65] The analogous pumping of metal atoms or rare gas-metal excimers (which have electronic states lying below rare-gas metastables or excimers) has been suggested.[66] In the Xe-Hg system, fluorescent emission bands, corresponding to perturbed emission from the 7^3S-6^3P normal atomic transitions of mercury (at 4047, 4358, and 5460 A) have been observed. The xenon metastables (at 8.3, 9.45 eV, and higher) preferentially excite the $Hg7^3S_1$ level at 7.75 eV on a faster time scale than the lower $^3P_{0,1,2}$ levels are excited by the Xe_2 excimer and produce an inversion on these transitions. At low partial pressures of mercury (~ 30 torr), emission bands (peaks at 2100 and 2700 A) from XeHg excimers are also observed. When the partial pressure of mercury is increased, XeHg excimer emissions decrease and are replaced by the emission from an even lower energy excimer, the mercury dimer.[66] The long radiative lifetime (~ 14 μs) and relatively small quenching losses[67] of the mercury excimer suggest that it will be useful as an energy storage reservoir for transfer to other radiative species.

Argon is the most generally useful of the rare gases for energy transfer. The somewhat larger ionization potential of argon (15.7 eV) compared to that of the heavier rare gases (~ 1.3 times that of xenon) corresponds to a higher energy of its excimer level, which permits resonant energy transfer from the argon excimer to krypton and xenon atoms. In the XeF and KrF lasers, the largest laser output is obtained with several atmospheres of the argon buffer and low partial pressures of xenon or krypton. This mixture has generally been interpreted as indicating that ground-state argon deactivates the rare gas-halogen excimer much less than xenon or krypton. The smaller excimer quenching by argon more than compensates both for the slightly lower conversion efficiency of deposited beam energy in argon (due to its larger ionization potential) and for the less-than-perfect (but very high) energy-transfer efficiency.[66] In the XeBr excimer laser, the use of argon/xenon mixtures rather than xenon will probably only improve laser action, because the observed cutoff at high pressures has been attributed to photoabsorption of laser emission by the Xe_2^* excimer.[49]

Argon is also the buffer gas used with an iodine donor molecule in the gas mixture of the I_2 laser. The reaction kinetics leading to I_2 formation in this system are relatively complicated. The I^- ions required in reactions (4) are produced by dissociative attachment of low-energy electrons to the iodine donor molecules CI. The positive ions I^+ and CI^+ are formed directly by Ar^+ and Ar_2^+ in charge-exchange reactions or by Ar^* and Ar_2^* in Penning ionization. However, the reaction kinetics require further study to identify the production mechanism in complete detail.

After the start of the e-beam pulse, the time required to reach the threshold inversion density ΔN_t for laser oscillation depends on the speed of the reaction kinetics that govern the flow of energy from the

primary beam excitation to the excimer level. The growth of population density in the upper level during pumping can be monitored by the fluorescent side emission from the optical cavity, which is relatively unaffected by photoabsorption and is essentially proportional to the excited-state density. With increase of the gas pressure, collisional energy transfers speed up and the time delay for the onset of laser emission decreases. As already discussed, laser efficiency and output increase with pressure up to an optimum value for a given gas mixture.

In a low gain system, the time required for the growth of observable laser emission from the spontaneous emission background is appreciable. Lasers operating slightly above oscillation threshold, with a large time delay between the peak of fluorescent emission and the peak of amplified spontaneous emission, show a highly nonlinear dependence of laser emission on the pumping rate. During the buildup of laser emission, the transient inversion density rises above the threshold value ΔN_t and is not saturated to a steady value $\approx \Delta N_t$ by the stimulated emission until the laser intensity has attained its potential steady level. As a consequence of the slow growth of laser intensity, the loss of upper-level energy in a low-gain laser through collisional and fluorescent decay can be high. The excimer decay rate may be high enough to dissipate much of the inversion energy and thus to terminate stimulated emission well before the oscillation level can reach the steady intensity that balances the pumping power input. Under these conditions the laser pulse peaks long after ($\gtrsim$ 50 ns) the fluorescent emission, has a very short temporal duration, and has a low efficiency.

In a high-gain system, the laser turns on soon after the e-beam reaches full power and quickly thereafter attains the steady intensity at which inversion density is held near the threshold value ΔN_t. The loss of inversion energy from quenching of the upper laser level is thereby kept to a minimum. Provided there is no buildup of population in the lower level and no blocking of laser action by the growth of absorbing species, the laser intensity continues steady with the pulse level until beam turnoff. On the other hand, bottlenecking in the lower level reduces the extractable power from the excimer energy and causes a steady decline of laser intensity. The production of an absorbing species in the reaction chain may also result in early termination of the laser pulse.

The efficiency attainable in the KrF laser can be estimated from the approximate efficiencies anticipated in the various energy-transfer processes. In the slowing-down of energetic electrons, the average electron energy transferred to the stopping material (by primary beam electrons and by the cascade of energetic secondary electrons) per ion pair produced is almost independent of the energy of the primary electron. For fast electrons in argon gas, the average energy deposited in the medium per ion pair is 26.2 eV, of which on the average 22.6 eV is expended to produce an argon ion and the remaining 3.6 eV is left as excitation of argon atoms, with one argon atom produced at a mean excitation of 13.2 eV per 3 5 ions. Practically every argon ion ends up as an excited neutral atom by molecular ion formation and recombination, so that ~20.5 eV of electron energy is used for each metastable Ar* (~ 11.5 eV) created. Energy transfer from Ar* to krypton appears to occur with almost 100% efficiency.[68] The small amount of krypton in the mixture ($\lesssim$ 10%) can also be excited directly into Kr* by the electron beam (with somewhat less average energy) through the processes analogous to those in argon. The large cross section of the Kr* + CF reaction and the favorable yield of KrF excimer (the measured branching ratio is near unity in the analogous Xe* + $F_2 \rightarrow$ XeF* + F reaction[54]) indicate that most of the krypton metastable energy can

be transferred to the excimer KrF*. The measured rate for formation of KrF* from the reaction $Kr^* + NF_3$ is 26×10^{-11} $cm^3 \cdot s^{-1} \cdot mol^{-1}$. In general, fluorine donors with the minimum bond-dissociation energy produce the excimer most efficiently.[55]

If lasing action is not blocked by reaction products and if bottlenecking in the lower laser level does not occur, the laser emission can extract all the excimer energy produced by the e-beam excitation beyond the excimer energy lost by decay in maintaining the threshold inversion. The KrF system appears to be free of both of these undesirable properties, as well as having negligible photoabsorptive losses by the excimer or donor molecule at the lasing frequency.

The KrF laser radiation at 2485 Å corresponds to a photon energy of 5.03 eV. About 20.5 eV of e-beam energy is required to produce an argon metastable, which may result in a KrF* excimer, so the quantum efficiency is about 24%. An estimate of the energy transfer efficiency in excimer production from argon metastables is 50% at the optimum pressure (a few atmospheres) for the gas mixture. Hence a KrF laser operating well above the threshold region is expected to show an efficiency up to 12%. For the fast rise time (~ 10 ns) e-beam pulses required for these lasers, state-of-the-art design for pulse forming networks can achieve an efficiency of ~ 75% (ratio of electron kinetic energy emerging from e-beam gun to energy stored in capacitors). It is anticipated that axial e-beam excitation can ultimately attain uniform deposition of ~ 90% of the e-beam energy in the optical cavity, which would result in an overall electrical to optical efficiency of ~ 8%.

The highest output pulse energy obtained at this time with the KrF system is 117 J in a 55-ns pulse with peak power ~ 1.7×10^9 W and laser efficiency of ~ 3.5%.[57] About 3.2 kJ of e-beam energy were deposited within the optical region in a mixture of $Ar:Kr:F_2$ at partial pressures of 3000:150:6 torr. At low krypton pressures, laser emission from the ArF excimer transition occurred simultaneously with KrF emission. At a krypton partial pressure of 25 torr, half the laser energy output was from ArF, but above 100 torr the ArF emission ceased. In an $Ar:F_2$ mixture under the same e-beam bombardment conditions, laser pulses up to 92 J with peak power ~ 1.3×10^9 W at the same 3.5% efficiency were obtained. These results indicate that in the reaction kinetics of the KrF laser, excimer production by excimer exchange (3b) with (ArF*) is important.

The average power from a pulsed laser is equal to the product of pulse energy and pulse repetition rate. The high peak powers obtainable from the high-gain excimer lasers indicate that repetition rate will dominate their average power output. The single-pulse energy of an e-beam-pumped laser is limited mainly by the pinching of the beam due to its magnetic self-field, which for a given current density (A/cm^2) constrains the transverse dimensions of the beam. Beam pinching is believed to impose a limitation on beam currents to $\lesssim$ 200 kA or on magnetic fields $\lesssim$ 1 kG. The limit on total beam current places an ultimate limitation on the gas volume that can be pumped and hence on the total pulse energy.

The principal constraint on the repetition rate of e-beam-pumped lasers is beam heating of the foil separating the electron-gun vacuum chamber from the high-pressure gas cell. The foil is bombarded by pulses of relativistic electrons at current densities of hundreds of amperes per square centimeter for pulse durations of 50 ns or more. Although thermal loads of 100 W/cm^2 have been sustained in small beam foils,[70] current state-of-the-art for large area beams limits the maximum average power deposition in the foil to about 10 W/cm^2. With a 200-A/cm^2, 100-ns e-beam pulse that loses 40 keV energy in the foil, the upper limit to the pulse repetition rate is

~ 10 pps. Increases much beyond this rate may not be possible unless significant progress in foil cooling technology is made.

Electric-Discharge-Excited Excimer Lasers

Demonstration experiments and scaling investigations of laser action in excimer systems to date have used e-beam pumping. However, the bimolecular formation processes (2) of the rare gas-monohalide excimers permit laser operation at sufficiently low pressures that excitation by fast electric discharge is possible. Recently, a few of these lasers, the high-gain KrF and XeF systems, have been operated successfully by electric-discharge excitation. As yet, discharge excitation has been accomplished for relatively small (~ 10 to 100 mJ) devices, but this approach is now under active development. An extensive technology base exists for high-pressure ($\geq$ 1 atm) gas-laser systems excited by pulsed transverse discharge, and available state of the art can be applied to the excimer systems.[32]

Electric-discharge pumping (EDP) offers the promise of much higher average power and somewhat greater efficiency than e-beam pumping (EBP). Even with e-beam-controlled discharge, the primary beam current densities are less than one-tenth those in EBP and foil-heating limits on average laser power are greatly reduced. In addition, the total pulse energy obtainable from a single laser unit may be greater for self-sustained EDP, because the limitation on gas volume imposed by e-beam pinching does not apply.

The efficiency of converting capacitor-stored electrical energy to energy deposited in rare-gas metastable atoms may be higher for EDP. Electrical pulse generation tends to be more efficient at the lower voltages used in discharges. Also, electrical energy is transferred (by the conduction current) only to the gas in the volume defined by the discharge electrodes; good matching with the load impedance in the discharge is usually possible. Even with an e-beam sustainer, electron energy losses in penetrating the foil and scattering out of the optical volume constitute only a small fraction of the total electrical energy. Moreover, Boltzmann-equation calculations of metastable production by electrons in a discharge plasma predict efficiencies of ~ 70% of the deposited energy.[70] The potentially greater metastable production efficiency in EDP compared to ~ 50% in EBP is a result of the larger fraction of energy-efficient direct atomic excitation compared to atomic ionization in a stabilized discharge.

The most serious limitation on laser energy with EDP is imposed by the allowable density of metastables that can be sustained under stable discharge. The energy required to ionize an excited rare-gas atom is much less than the excitation energy of the atom. Moreover, the cross section for electron-impact ionization of the excited atom is usually much larger than the cross section for ground-state excitation. Hence, lower-energy electrons in the discharge plasma can readily ionize rare-gas metastables. There are many more of these lower-energy electrons than there are electrons in the high-energy tail of the distribution that produce the ground state excitation. When the metastable density is sufficiently large, impact ionization of metastables will dominate the electron energy-loss processes and will lower the efficiency. Steady controlled discharge is impossible for electric fields large enough to build up metastable densities at which metastable ionization can avalanche and produce arcing. Initial studies indicate that EDP of metastables other than rare gases such as mercury, are much less limited by allowable metastable densities in the discharge.

In e-beam-controlled EDP, the KrF system has used a gas mixture with an argon buffer (~ 98%) and a few percent krypton. Let us anticipate that 70% of the energy

deposited in the gas is channelled into rare-gas metastables Ar* (~ 11.5 eV) and Kr* (~ 9.9 eV) in the KrF system. If the energy-transfer efficiency from metastables to KrF excimers is 50%, then laser emission (5.03-eV photons) well above the threshold region can attain an efficiency up to ~ 15%. An anticipated efficiency of 80% in the pulse-discharge circuit would result in an overall electrical-to-optical efficiency of ~ 12% in this system. The main uncertainty in realizing efficiencies of this magnitude centers on achieving the large excimer densities required for laser operation in the region of efficient hig.-energy output.

Laser action has been achieved with pulsed e-beam controlled discharge pumping of the KrF system.[70] A mixture of 0.1:2.0:97.9::F_2:Kr:Ar lased at total pressures ranging from 0.75 to 3 atm, but when self-sustained (no e-beam) discharge in the mixture was attempted, arc discharge always occurred immediately with no observable laser emission. Optimum laser performance was obtained at 1 atm and a discharge electric field of 3 kV/cm with a 90-ns (FWHM) pulse of 4 mJ energy at an efficiency of ~ 0.2%. Efficiency is defined as the ratio of laser output energy to discharge energy deposited in the gas during the controlled (no arcing) portion of the discharge pulse. It is estimated that under these conditions, efficiency can be increased to 1% by optimizing the optical output coupling and eliminating photoabsorption of the laser beam by F_2 in traversing the large length of gas mixture outside the discharge volume (2 by 20 by 2 cm).

In these experiments, the discharge was initiated ~ 35 ns after turnon of the 135-ns (~ 25 ns rise time) e-beam pulse (150 keV, 8 A/cm^2, 2 by 20 cm). The discharge is controlled by e-beam ionization until beam turnoff, followed by a transitional period, and terminates with the onset of arc discharge. The "stable" portion of the discharge pulse extends up to the start of discharge arcing. In the e-beam-sustained discharge, plasma impedance is much lower than circuit impedance (which includes a series resistor to protect the laser cavity by absorbing the capacitor energy during arc discharge). During this time (~ 100 ns) the discharge voltage remains nearly constant and the discharge current builds up (E ~ 3 kV/cm and peak I ~ 100 A/cm^2 at 1 atm, 0.2% efficiency). The transitional discharge begins with e-beam turnoff: rapid attachment of discharge electrons to F_2 causes the plasma resistivity to increase; the inductive increase in voltage across the gas due to the changing discharge current results in eventual avalanche ionization of metastables and arcing. Operation of the controlled discharge at larger electric fields, with attendant larger discharge currents, causes larger inductive voltages after e-beam turnoff and faster transition to arc discharge. However, increased pumping power produces a larger inversion density and reduces the onset lag, defined as the time interval between discharge turnon and the onset of laser emission. With increasing pumping power, laser efficiency rises rapidly after oscillation threshold is reached, peaks at some value of the discharge electric field, and then with further increase of electric field, rapidly decreases (probably from the losses accompanying high metastable ionization at large metastable densities) even though total energy output increases somewhat. With increasing gas pressure (minimum operable pressure, ~ 0.75 atm), gas kinetics speed up and both the onset lag and the laser-pulse duration are reduced. Laser output in this small system always peaked after the stable portion of the discharge, indicating an absence of bottlenecking (as expected for a bound-free transition).

Self-sustained electric discharge pumping of a XeF excimer laser has been demonstrated.[71] In this approach, a stable discharge is maintained throughout the discharge

period by (1) shortening the discharge time (in this case, 30 ns with a 20-ns risetime) relative to the arc-formation time, and (2) limiting the discharge-current density by using a large discharge area and a small discharge length. Laser emission was obtained in mixtures of $He:Xe:NF_3$ at total pressures between 300 and 1000 torr Maximum laser energy of 7 mJ was obtained from a $0.5:1.5:98::NF_3:Xe:He$ mixture at a total gas pressure of 300 torr. Maximum energy output was obtained with pressures between 300 and 600 torr, if the partial pressure of NF_3 remained at about 1 torr. The electrical-to-optical efficiency was ~ 0.1%. The laser pulse had a width of ~ 20 ns and always began near the end of the current pulse. The long onset lag indicates laser operation near the threshold region. Because the XeF excimer has a large cross section for stimulated emission, the slow buildup of gain must be attributed to the kinetics of excimer formation in the discharge.

Comparable laser performance was obtained when neon was substituted for helium. But when argon was used as the buffer gas, rapid arc formation with no laser emission was observed. Arcing in the discharge also occurred when the proportion of xenon in the mixture exceeded 10%. The higher metastable energies (helium, 19.8 eV, neon, 16.6 eV) and the larger ionization energies of the helium and neon metastables (larger by ~ 1 eV) compared to the metastables of heavier rare gases inhibit metastable formation and ionization of the buffer gas in the discharge. In the discharge the electrons experience essentially only elastic collisions with the buffer (helium or neon) gas, which thus serves mainly to equilibrate and distribute the electrons uniformly and thus to stabilize the discharge. The observed decrease in energy output for NF_3 concentrations above 0.5% probably arises from quenching of the XeF excimer by NF_3.

With no gas flow through the cell, laser energy began to fall off after ~ 10 pulses. The likely cause is NF_3 depletion due to production of free fluorine in the discharge (excited neutrals by dissociative excitation of NF_3 or ions by dissociative electron attachment) and its subsequent reaction with cell materials. With gas flow through the cell, stable pulse repetition was demonstrated up to 10 Hz in this system. With a fixed gas flow rate, the average pulse energy begins to decrease rapidly as the repetition rate is increased above the stable level. This results from NF_3 depletion and indicates an optimum flow rate for a given pulse rate. The superior efficiency of the XeF system compared to the N_2 laser (3371 Å) is indicated by the maximum laser pulse energy, 3.5 mJ, produced by the same apparatus with an $N_2:SF_6$ mixture.

With a similar gas mixture a smaller XeF system has produced laser emission in self-sustained fast discharge at pressures between 200 and 400 torr.[72] The 1-mJ pulses of ~ 40-ns width were obtained at 350 torr total pressure with an electrical-to-optical efficiency of 0.2% using a Blumlein fast-pulse generator. At the pressures required, a more uniform transverse discharge is obtained with the fast Blumlein-type circuitry. The absence of laser emission below 200 torr is attributed to the slow vibrational relaxation of the excimer level, as shown by the large frequency spread of the fluorescent emission at the low pressures. Above 200 torr, laser output energy increases with pressure and reaches a maximum at 400 torr. With further increase of pressure, excessive arcing with resultant lowered output occurs. At the low concentrations of xenon metastables and excimers that prevail in this experiment, a simple model predicts the observed excimer density and threshold gain. The electron density and mean velocity are estimated from the measured discharge

voltage, current, and pressure. In the simplified kinetics of the model, it is assumed that

- the only roles played by the buffer molecules are to help maintain a uniform discharge by elastic scattering of the discharge electrons and to relax the excimer vibrational energy by two-body collisions,
- excimer formation is dominated by the bimolecular process (2), and
- excimer loss occurs mainly by radiative decay.

Laser action has also been achieved for KrF by unaided Blumlein-type fast-discharge devices.[73,74] Careful design of the discharge electrodes dramatically improves discharge uniformity and efficiency. However, for both XeF and KrF, preionization vastly increases (by 30 to 50%) the maximum laser energy output compared to the maximum obtainable without preionization.[74] Preionization improves uniformity of the discharge at higher pressures (~ 700 torr), so that optimized gas mixtures containing larger concentrations of fluorine donors (NF_3) at higher total pressures can be utilized. With a mixture of 1.2:1.2:97.6 (NF_3:Xe:He) at a total pressure of 750 torr, a XeF laser produced 4-ns pulses with maximum energy of 100 mJ at an overall efficiency of ~ 1%. Moreover, a linear increase of pulse energy with input energy, typical of pulsed lasers operating above saturation intensity, was observed. With the same device and a mixture of 0.1:6.0:93.9 (NF_3:Kr:He) laser pulses from KrF of ~ 25 ns (FWHM) and 30 mJ were obtained at 0.3% efficiency, and most recently performance on KrF has been improved to 130-mJ pulses at greater than 1.0% overall efficiency.[75] The difference in pulse shapes between the XeF and KrF is probably due to differences in kinetic rates and in stimulated-emission cross sections.

The more direct kinetics of excimer production in self-sustained discharges imply that the projected efficiency for this type of laser operation is somewhat higher than for e-beam-controlled discharges. For the KrF system, direct metastable production of Kr^* (9.9 eV) gives a quantum efficiency for laser emission (5.03-eV photons) of ~ 50%. If metastables are produced from discharge-energy deposition with 70% efficiency, and subsequent excimer formation kinetics occur with 75% efficiency, then an ultimate laser efficiency of ~ 26% is obtained. An 80% efficiency in the discharge for depositing the capacitor-stored energy into the gas gives an overall electrical to optical efficiency of ~ 21%. However, scaling of the discharge-pumped excimer lasers to very high energy outputs may require e-beam control of the discharge.

The pulse energy, average power, and overall efficiency that can ultimately be obtained from discharge-pumped excimer lasers depend on their scaling properties to larger gas volumes and gain lengths, which are necessary for efficient high-energy output. At present e-beam pumping is much further advanced in demonstrated scalability to high energies. With discharge excitation, the e-beam-controlled version appears to have the greater potential for large pulse energy and average power. However, the greater simplicity of self-sustained discharge systems encourages their further development for many applications. In all these systems, high repetition rate and large average power will require fast gas flow to remove from the optical cavity the heat and side products generated in the excitation kinetics. Extensive experience with rapid gas recirculation in large lasers such as CO_2 is available for application to the newer systems.[32,76] Further research in basic kinetics, and the development of operating techniques and devices for excimer lasers, will provide the experimental data and detailed modeling that fully characterize the performance to be realized from these systems.

REFERENCES

1. R. S. Mulliken, "Potential Curves of Diatomic Rare-Gas Molecules and their Ions, with Particular Reference to Xe_2^*," J. Chem. Phys. 52, 5170-5180 (1970).

2. H. A. Koehler, L. J. Ferderber, D. L. Redhead, and P. J. Ebert, "Stimulated vuv Emission in High-Pressure Xenon Excited by High-Current Relativistic Electron Beams," Appl. Phys. Lett. 21, 198-200 (1972).

3. G. Herzberg, Spectra of Diatomic Molecules, 2nd Ed. (D. Van Nostrand Company, Inc., New York, 1950), Chap. VII.

4. D. J. Eckstrom, R. M. Hill, R. A. Gutcheck, D. L. Huestis, and D. C. Lorents, "Studies of E-Beam Pumped Molecular Lasers," Stanford Research Institute Semiannual Technical Report No. 2, SRI MP73-1 (July 1973).

5. J. E. Velazco and D. W. Setser, "Bound-Free Emission Spectra of Diatomic Xenon Halides," J. Chem. Phys., 62, 1990-1991 (1975).

6. J. J. Ewing and C. A. Brau, "Emission Spectrum of XeI* in Electron-Beam-Excited Xe/I_2 Mixtures," Phys. Rev., A12, 129-132 (1975).

7. C. A. Brau and J. J. Ewing, "Emission Spectra of XeBr, XeCl, XeF, and KrF," J. Chem. Phys., 63, 4640-4647

8. R. S. Mulliken, "Iodine Revisited," J. Chem. Phys. 55, 288-309 (1971).

9. J. Tellinghuisen, "The McLennon Bands of I_2: A Highly Structured Continuum," Chem. Phys. Lett. 29, 359-363 (1974).

10. M. V. McCusker, R. M. Hill, D. L. Hvestis, D. C. Lorents, R. A. Gutcheck, and H. H. Nakano, "The Possibility of an Efficient Tunable Molecular Iodine Laser Near 340 nm," Appl. Phys. Lett. 27, 363-365 (1975).

11. J. J. Ewing and C. A. Brau, "Laser Action on the 342-nm Molecular Iodine Band," Appl. Phys. Lett. 27, 557-559 (1975).

12. R. S. Bradford, Jr., E. R. Ault, and M. L. Bhaumik, "High-Power I_2 Laser in the 342-nm Band System," Appl. Phys. Lett. 27, 546-548 (1975).

13. A. K. Hays, J. M. Hoffman, and G. C. Tisone, "25 Megawatt Molecular-Iodine Laser,"

14. C. D. Cooper, G. C. Cobb, and E. L. Tolnas, "Visible Spectra of XeO and KrO," J. Mol. Spectrosc. 7, 223-230 (1961).

15. G. C. Tisone, "Lifetime and Quenching Rate Constants of the Green Bands of XeO," J. Chem. Phys. 60, 3716-3717 (1974).

16. H. T. Powell, J. R. Murray, and C. K. Rhodes, "Laser Oscillation on the Green Bands of XeO and KrO," Appl. Phys. Lett. 25, 730-732 (1974).

17. D. L. Huestis, R. A. Gutchek, R. M. Hill, M. V. McCusker, and D. C. Lorents, "Studies of E-Beam Pumped Molecular Lasers," Stanford Research Institute Technical Report No. 4, SRI NOMP75-18 (January 1975).

18. J. C. W. Johns, "A Spectrum of Neutral Argon Hydride," J. Mol. Spec. 36 488-510 (1970).

19. V. Bondybey, P. K. Pearson, and H. F. Schaefer III, "Theoretical Potential Energy Curves for OH, HF^+, HF, HF^-, NeH^+, and NeH," J. Chem. Phys. 57, 1123-1128 (1972).

20. C. G. Freeman, M. J. McEwan, R. F. C. Claridge, and L. F. Philips, "The Reactions of Xenon and Mercury with $Hg(^3Po)$," Chem. Phys. Lett. 6, 482-484 (1970).

21. O. P. Strausz, J. M. Campbell, S. DePaoli, H. S. Sandhu, and H. E. Gunning, "Band Fluorescence Spectra in Mercury $6(^3P_1)$ Photosensitization," J. Am. Chem. Soc. 95, 732-739 (1973).

22. C. G. Freeman, M. J. McEwan, R. F. C. Claridge, and L. F. Philips, "Mercury-Sensitized Luminescence of H_2O and D_2O," Trans. Faraday Soc. 66, 2974-2979 (1970).

23. R. H. Newman, C. G. Freeman, M. J. McEwan, R. F. C. Claridge, and L. F. Philips, "Mercury-Sensitized Luminescence of NH_3 and ND_3," Trans. Faraday Soc. 66, 2827-2836 (1970).

24. A. V. Phelps, "Tunable Gas Lasers Utilizing Ground State Dissociation," Joint Institute for Laboratory Astrophysics report No. 110 (September 1972).

25. G. York and A. Gallagher, "High Power Gas Lasers Based on Alkali-Dimer A-X Band Radiation," Joint Institute for Laboratory Astrophysics report no. 114, University of Colorado (October 1974).

26. A. Tam, G. Moe, W. Park, and W. Happer, "Strong New Emission Bands in Alkali-Noble-Gas Systems," Phys. Rev. Lett. 35, 85-87 (1975).

27. J. G. Eden, J. T. Verdeyen, and B. E. Cherrington, "Optical Absorption and Emission in High Pressure Cs-Xe Mixtures," Bull. Am. Phys. Soc. 21, 168 (1976).

28. J. Pascale and J. Vandeplanque, "Excited Molecular Terms of the Alkali-Rare Gas Atom Pairs," J. Chem. Phys. 60, 2278-2289 (1974).

29. A. C. Tam, G. Moe, B. R. Bulos, and W. Happer, "Excimer Radiation from Na-Noble-Gas and K-Noble-Gas Molecules," Opt. Commun. 16, 376-379 (1976).

30. C. H. Chen and M. G. Payne, "A Potential High-Efficiency Cl_2 Ultraviolet Laser," Appl. Phys. Lett. 28, 219-221 (1976).

31. R. M. Hill, D. L. Huestis, and C. K. Rhodes, "Review of High Energy Visible and UV Lasers," in Physics of Quantum Electronics vol. 3, S. F. Jacobs, M. O. Scully, and M. Sargent III, Eds. (Addison-Wesley, Reading, 1976).

32. O. R. Wood, II, "High-Pressure Pulsed Molecular Lasers," Proc. IEEE 62, 355-397 (1974).

33. C. K. Rhodes, "Review of Ultraviolet Laser Physics," IEEE J. Quantum Electron. QE-10, 153-174 (1974).

34. J. R. Murray and P. W. Hoff, "Lasers for Fusion," in Physics of Quantum Electronics Vol. 1, S. F. Jacobs, M. O. Scully, and M. Sargent III, Eds. (Addison-Wesley, Reading, 1974).

35. S. C. Wallace and R. W. Dreyfus, "Continuously Tunable Xenon Laser at 1720 Å," Appl Phys. Lett. 25, 498-500 (1974).

36. R. J. Carbone and M. M. Litvak, "Intense Mercury-Vapor Green-Band Emission," J. Appl. Phys. 39, 2413-2416 (1968).

37. D. J. Eckstrom, R. M. Hill, D. C. Lorents, and H. H. Nakano, "Collisional Quenching and Radiative Decay of the Mercury Excimer," Chem. Phys. Lett. 23, 112-114 (1973).

38. R. M. Hill, D. J. Eckstrom, D. C. Lorents and H. H. Nakano, "Measurements of Negative Gain for Hg_2 Continuum Radiation," Appl Phys. Lett. 23, 373-374

39. A. J. Palmer, "Stimulated Emission of the H_2 Continuum," J. Appl. Phys. 41, 438-439 (1970).

40. J. B. Gerardo and A. Wayne Johnson, "High-Pressure Xenon Laser at 1730 Å," IEEE J. Quantum Electron. QE-9, 748-755 (1973).

41. J. B. Gerardo and A. Wayne Johnson, "1730-Å Radiation Dominated by Stimulated Emission from High-Pressure Xenon," J. Appl. Phys. 44, 4120-4124 (1973).

42. W. M. Hughes, J. Shannon, A. Kolb, E. Ault, and M. Bhaumik, "High-Power Ultraviolet Laser Radiation from Molecular Xenon," Appl. Phys. Lett. 23, 385-387 (1973).

43. P. W. Hoff, J. C. Swingle, and C. K. Rhodes, "Observations of Stimulated Emission from High-Pressure Krypton and Argon/Xenon Mixtures," Appl. Phys. Lett. 23, 245-246 (1973).

44. A. Wayne Johnson and J. B. Gerardo, "Diluent Cooling of a Vacuum-Ultraviolet High-Pressure Xenon Laser," J. Appl. Phys. 45, 867-872 (1974).

45. W. M. Hughes, J. Shannon, and R. Hunter, "Efficient High-Energy-Density Molecular Xenon Laser," Appl. Phys. Lett. 25, 85-87 (1974).

46. W. M. Hughes, J. Shannon, and R. Hunter, "126.1 nm Molecular Argon Laser," Appl. Phys. Lett. 24, 488-490 (1974).

47. W. M. Hughes, N. T. Olson, and R. Hunter, "Experiments on 558-nm Argon Oxide Laser System," Appl. Phys. Lett. 28, 81-83 (1976).

48. S. K. Searles and G. A. Hart, "Stimulated Emission at 281.8 nm from XeBr," Appl. Phys. Lett. 27, 243-245 (1975).

49. S. K. Searles, "The XeBr Excimer Laser," (to be published).

50. J. J. Ewing and C. A. Brau, "Laser Action on the $^2\Sigma^+_{1/2} \rightarrow {}^2\Sigma^+_{1/2}$ Bands of KrF and XeCl," Appl. Phys. Lett. 27, 350-352 (1975).

51. C. A. Brau and J. J. Ewing, "354-nm Laser Action on XeF," Appl. Phys. Lett. 27, 435-437

52. E. R. Ault, R. S. Bradford, Jr., and M. L. Bhaumik, "High-Power Xenon Fluoride Laser," Appl. Phys. Lett. 27, 413-415 (1975).

53. G. C. Tisone, A. K. Hays, and J. M. Hoffman, "100 MW, 248.4 nm, KrF Laser Excited by an Electron Beam," Opt. Commun. 15, 188-189 (1975).

54. M. L. Bhaumik, R. S. Bradford, Jr., and E. R. Ault, "High-Efficiency KrF Excimer Laser," Appl. Phys. Lett. 28, 23-24 (1976).

55. G. C. Tisone, A. K. Hays, and J. M. Hoffman, "Studies of Rare-Gas-Halogen Molecular Lasers Excited by an Electron Beam," presented at 2nd Summer Colloquium on Electronic Transition Lasers, (Woods Hole, MA, September 17-19, 1975).

56. J. Tellinghuisen, J. M. Hoffman, G. C. Tisone, and A. K. Hays, "Spectroscopic Studies of Diatomic Noble Gas Halides: Analysis of Spontaneous and Stimulated Emission from XeCl," J. Chem. Phys. 64, 2484-2490 (1976).

57. J. M. Hoffman, A. K. Hays, and G. C. Tisone, "High Power UV Noble-Gas-Halide Lasers," Appl. Phys. Lett. 28, 538-539 (1976).

58. D. C. Lorents and R. E. Olson, "Excimer Formation and Decay Processes in Rare Gases," Stanford Research Institute Semiannual Technical Report No. 1, SRI Project 2018 (December 1972).

59. D. C. Lorents, D. J. Eckstrom, and D. Huestis, "Excimer Formation and Decay Processes in Rare Gases," Stanford Research Institute report MP73-2 (September 1973).

60. R. M. Hill, R. A. Gutcheck, D. L. Huestis, D. Mukherjee, and D. C. Lorents, "Studies of E-Beam pumped Molecular Lasers," Stanford Research Institute report MP74-39 (July 1974).

61. E. V. George and C. K. Rhodes, "Kinetic Model of Ultraviolet Inversions in High-Pressure Rare-Gas Plasmas," Appl. Phys. Lett. 23, 139-141 (1973).

62. P. W. Hoff, J. C. Swingle, and C. K. Rhodes, "Dynamic Model of High Pressure UV Lasers," IEEE J. Quantum Electron. QE-10, 775 (1974).

63. C. W. Werner, E. V. George, P. W. Hoff, and C. K. Rhodes, "Dynamic Model of High-Pressure Rare-Gas Excimer Lasers," Appl. Phys. Lett. 25, 235-238 (1974).

64. S. K. Searles and G. A. Hart, "Laser Emission at 3577 and 3805 Å in Electron-Beam-Pumped Ar-N_2 Mixtures," Appl. Phys. Lett. 25, 79-82 (1974).

65. E. R. Ault, M. L. Bhaumik, and N. T. Olson, "High-Power Ar-N_2 Transfer Laser at 3577 Å," IEEE J. Quantum Electron. 10, 624-626 (1974).

66. R. A. Gutcheck, R. M. Hill, D. L. Huestis, D. C. Lorents, and M. V. McCusker, "Studies of E-Beam pumped Molecular Lasers," Stanford Research Institute report MP75-43 (August 1975).

67. S. Penzes, H. S. Sandhu, and O. P. Strausz, "Kinetics of the 'a' and 'b' Band Emissions of Mercury Excimers with Added Gases," Int. J. Chem. Kinet. 4, 449-461 (1972).

68. L. G. Piper, D. W. Steser, and M. A. A. Clyne, "Electronic Energy Transfer from Metastable Argon Atoms to Krypton Atoms," J. Chem. Phys. 63, 5013-5028 (1975).

69. H. J. Jansen and P. N. Wolfe, private communication.

70. J. A. Mangano and J. H. Jacob, "Electron-Beam-Controlled Discharge Pumping of the KrF Laser," Appl. Phys. Lett. 27, 495-497 (1975).

71. R. Burnham, N. W. Harris, and N. Djeu, "Xenon Fluoride Laser Excitation by Transverse Discharge," Appl. Phys. Lett. 28, 86-87 (1976).

72. C. P. Wang, H. Mirels, D. G. Sutton, and S. N. Suchard, "Fast-Discharge-Initiated XeF Laser," Appl. Phys. Lett. 28, 326-328 (1976).

73. D. G. Sutton, S. N. Suchard, O. L. Gibb, and C. P. Wang, "Fast-Discharge-Initiated KrF Laser," Appl. Phys. Lett. 28, 522-523 (1976).

74. R. Burnham, F. X. Powell, and N. Djeu, "Efficient Electric Discharge Lasers in XeF and KrF," Appl. Phys. Lett. (to be published).

75. N. Djeu, private communication.

76. G. S. Dzakowic and S. A. Wutzke, "High-Pulse-Rate Glow-Discharge Stabilization by Gas Flow," J. Appl. Phys. 44, 5061-5063 (1973).

IV. CHARACTERISTICS OF TUNABLE IR LASERS

The ir spectrum is characterized by several very attractive high-power and high-efficiency lasers, e.g., the CO_2, CO, and HF laser systems. Each, while not tunable, can be made to lase on a number of discrete lines over a reasonable range. The range may be extended by isotropic substitution, as in the DF laser. One or more of the lasing lines of one of these lasers may be utilized in some isotope operation or photochemical applications. However, in general, where tunability is desired, other types of lasers or frequency shifting devices must be considered.

General classes of tunable ir lasers include:

- Semiconductor lasers covering 0.6 to 34 μm;
- Spin-flip Raman lasers covering 5 to 6 μm (CO laser-pumped) and 9 to 14 μm (CO_2 laser-pumped), with other frequencies possible with other pumping lasers;
- Nonlinear optical devices such as,
  - optical parametric oscillators with wavelength coverage from ~ 1 to 16 μm;
  - difference-frequency generators covering 2 to 6 μm;
  - two- or four-photon mixers covering 2 to 24 μm;
- Gas lasers, such as Zeeman-tuned lasers covering 3 to 9 μm and high-pressure CO_2 lasers covering 9 to 11 μm.

Semiconductor Diode Lasers

Semiconductor diode lasers have become a major class of tunable lasers since stimulated emission has been first observed

in GaAs in 1962. Stimulated emission has been obtained from direct band-gap semiconductors by optical or e-beam excitation, by forward-biased p-n junction injection, and by carrier generation via avalanche multiplication. The injection (diode) lasers (SDL) are the simplest to operate, are the smallest known lasing devices, and have received the widest application. There is a large literature on diode lasers. Literature reviews have been published by Adams and Landsberg,[1] Stein,[2] Kressal,[3] and more recently by Colles and Pidgeon,[4] and by Hinkley et al.[5]

Developments in heterojunction diodes have led to power-conversion efficiencies approaching 50% at low temperature. Most diode lasing is confined to cryogenic temperatures. However, continuous-wave operation has been obtained at 300 K with GaAs diodes producing about 100-mW average power.

The wavelength range over which a diode lases is determined by the composition of the material. Wavelength-tuning within the spectral range is accomplished by varying pressure, magnetic field, or temperature. These parameters affect the band-gap energy and the refractive index.

In the evaluation of the tuning range of SDL (and of SFR) lasers, the difference between spectral range and continuous tuning interval must be understood. The spectral range of a single diode represents the frequency or wave-number interval over which the laser can operate. In diode lasers, which have narrow gain spectra that can be tuned over relatively wide spectral intervals, cavity resonant frequencies are well separated. As the tuning parameter changes the cavity resonance and gain spectrum (at different rates) there are abrupt shifts in laser frequency known as "mode hop".

Mode hopping occurs with all three tuning methods. True continuous tuning is accomplished over limited ranges of 0.1 to 2 cm^{-1} by temperature variations mainly affecting the refractive index. The temperature variations are controlled by changing the current across the diode.

A list of diode and other semiconductor lasers is given in Table IX. The spectral ranges for several semiconductor lasers are shown in Fig. 8.

The major drawbacks of SDLs are low-temperature operation, limited lifetimes, and poor reliabilities. In addition, a major limitation for isotope separation or photochemistry is that average output power of tunable diodes is low (cw outputs of tunable diodes at 77 K are typically on the order of 10^{-5} W) requiring arrays of diode lasers to attain higher energy outputs. Table X summarizes selected diode laser characteristics.

Spin-Flip Raman Lasers

Interest in spin-flip Raman (SFR) lasers has been spurred by the development of high-power CO and CO_2 lasers, and by the desire to use these high-energy, but fixed-frequency laser outputs over a wide frequency range. Spin-flip Raman lasers are not primary lasers, but are really optically pumped frequency-conversion devices.

Stimulated spin-flip Raman scattering is characterized by inelastic (Raman) scattering of incident photons from mobile charge carriers in a semiconductor crystal. Scattering photons lose (Stokes shift) or gain (anti-Stokes shift) an amount of energy proportional to an applied magnetic-field strength, and tuning is accomplished by varying the magnetic field strength. Spin-flip Raman scattering has been observed in several materials, including n-type InSb, PbTe, and $Hg_xCD_{1-x}Te$.

The magnetic field strength needed for SFR scattering is largely dependent on the mobile charge-carrier concentration in the crystal. Typically, magnetic fields of 25 to 100 kG are reported. An InSb crystal with an electron density of $10^{16}/cm^3$ requires a minimum of 24 kG. Reducing the concentration reduces the magnetic field-strength requirement, and

TABLE IX

SPECTRAL RANGE COVERED BY SELECTED SEMICONDUCTOR LASERS (INCLUDING AVALANCHE BREAKDOWN, OPTICALLY PUMPED, E-BEAM PUMPED, AND INJECTION LASERS)

Lasing Material	Frequency (μm)	Pumping Method			
		Optical	E-Beam	Injection	Avalanche
ZnS	0.33	x	x	---	---
ZnO	0.37	---	x	---	---
ZnSe	0.46	---	X	---	---
CdS	0.49	x	x	---	---
ZnTe	0.53	---	x	---	---
GaSe	0.59	---	x	---	---
CdSe	0.675	x	x	---	---
CdTe	0.785	---	x	---	---
GaAs	0.83-0.91	x	x	x	x
InP	0.91	---	---	x	x
$CdSnP_2$	1.01	---	x	---	---
GaSb	1.55	---	x	x	---
Cd_3P_2	2.1	x	---	---	---
InAs	3.1	x	x	x	---
Te	3.72	---	x	---	---
PbS	4.3	---	x	---	---
InSb	5.2	x	x	x	x
PbTe	6.5	---	x	x	---
PbSe	8.5	---	x	x	---
PbSnTe	28.	---	---	x	---
PbSnSe	8.-34.	---	---	x	---

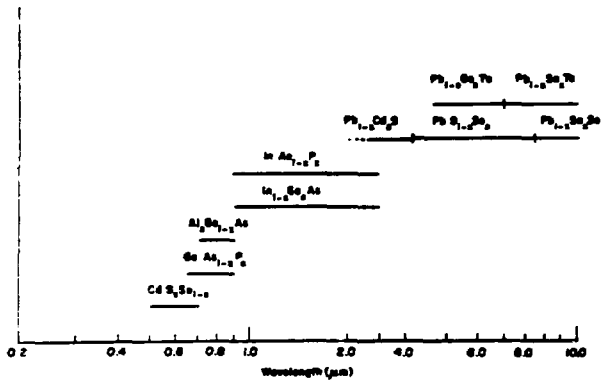

Fig. 8. Tuning ranges of semiconductor lasers.

TABLE X

CHARACTERISTICS OF DIODE (INJECTION) LASERS

Advantages - Wide spectral range, small size, high resolution, may be arrayed.

Disadvantages - Poor reliability, limited lifetime, low average power, requirement for cryogenic temperatures to obtain high efficiencies and high average power, mode-hopping.

Applications - Spectroscopy, communications.

Tuning Methods - Pressure, temperature, magnetic fields.

Operation - Predominantly cw, pulsed.

400 G is sufficient if the electron density in InSb is reduced to ~ $10^{15}/cm^3$. However, stimulated Raman power is also reduced at lower electron densities.

Continuous-wave operation of InSb is allowed when pumped with a CO laser at the temperature of boiling helium because the band-gap energy corresponds to a wavelength of 5.3 μm. High power (kilowatt range) and high conversion efficiencies (40 to 50%) are possible in pulsed operation at 5.3 μm with relatively low magnetic fields (900 G) using the frequency-doubled output of a CO_2 TEA laser.

While a spin-flip Raman laser is very valuable for spectroscopy applications, the requirements for cryogenic cooling and superconducting magnets will limit its use in laser-chemistry applications. Table XI summarizes selected SFR characteristics.

Optical Parametric Oscillators

An optical parametric oscillator (OPO) makes use of nonlinear optical effects caused by the interaction of three (or more) high-frequency electromagnetic waves to achieve a tunable emission. In a material with the necessary nonlinear ind . of refraction, a high-frequency, high-power, electromagnetic wave (the pump) interacts with a pair of lower-frequency (tunable) electromagnetic fields (called the signal and idle), amplifying them. The high-power pump field, in effect, modulates the linear dielectric constant seen by the lower-frequency waves, providing coupling between them.

TABLE XI

CHARACTERISTICS OF SPIN-FLIP RAMAN (SFR) LASERS

Advantages - Wide tuning range, very narrow linewidth,

Disadvantages - Liquid-helium cooling, superconducting magnet.

Applications - Spectroscopy, communications, nonlinear optical systems.

Tuning Method - Magnetic field.

Operation - Continuous wave (near 5.3 m), pulsed (5.3 or 10.6 m).

The low-frequency signals are tuned by rotating the nonlinear crystal, by changing the temperature of the crystal (and hence its refractive index), by applying pressure, or by applying electrical fields.

Theoretical efficiencies are high with internal conversion efficiencies approaching 100% for both singly resonant oscillators (SRO) and doubly resonant oscillators (DRO) in ring configurations. Net average power-conversion efficiencies between 10 and 45% have been reported for several pumping-laser and OPO combinations.[4,6] A conversion efficiency of ~ 70% has been reported for a Q-switched YAG:Nd laser and a $LiNbO_3$ OPO operating near 2.1 μm.[6]

The spectral tuning range for an OPO material is limited by the mirror coatings, by the basic transparency of the material, by the range of control of phase matching, or by an increase in threshold with longer-wavelength pump sources. Transparency ranges for prospective OPO materials are listed in Table XII. OPO operation has been observed to 11 μm with CdSe pumped by a Nd:YAG laser and beyond 16 μm with CdSe pumped by a HF laser.[7] Within the spectral range of an OPO material, the actual tuning is characterized by frequency hopping.

The OPO materials that have received most attention to date are CdSe, $LiNbO_3$, KDP, ADP, and $Ba_2NaNb_5O_{15}$. Procestite and pyringrite are being investigated. Important requirements for nonlinear OPO materials are that they (a) lack a center of symmetry, (b) possess a large figure of merit (Table XII), (c) are phase-matchable, (d) are transparent for all three frequencies, and (3) are homogeneous, of good optical quality, and resistant to damage above the operating threshold.

Two general types of OPOs are the doubly resonant oscillator (DRO) and the

TABLE XII

TRANSPARENCY RANGES FOR SELECTED OPO MATERIALS

Material	Figure of Merit[a]	Transparency Range (μm)
KDP[b]	0.4	0.25-1.2
ADP[c]	0.55	0.25-1.15
$LiIO_3$	28.	0.4-4
$LiNbO_3$	14.	0.4-4
$Ba_2NaNb_5O_{15}$	95.	0.4-4
Ag_3AsS_3[d]	50.	0.65-10
Ag_3SbS_3[e]	50.	0.70-10
CdSe	300.	1-20
HgS	500.	0.6-13
Se	10^4	0.8-25
Te	4×10^4	5-25

[a] $d^2/n^3 \times 10^{18}$ csu, where d is the second-order nonlinear coefficient and n is the index of refraction. A large value is desired.

[b] Potassium-dihydrogen phosphate.

[c] Ammonium-dihydrogen phosphate.

[d] Proustite.

[e] Pyrargrite.

singly resonant oscillator (SRO). The DRO is characterized by a low relative threshold, a single-mode pump bandwidth requirement, and relatively poor stability. The SRO has a relatively high threshold, multimode pump allowed, and good stability.

A major advantage of OPO frequency conversion relative to diode lasers and spin-flip is the room-temperature operation of the OPO. Selected characteristics of OPOs are summarized in Table XIII.

Other Nonlinear Techniques

Tunable ir laser outputs have been obtained by mixing a fixed-frequency laser beam with a tunable dye laser, both inputs operating in the visible. Pulsed laser outputs between 3 and 4 μm were observed when a tunable dye laser was mixed with a Q-switched ruby laser.[8]

Two- and four-photon mixing lasers have been demonstrated. Two-photon mixing

TABLE XIII

CHARACTERISTICS OF OPTICAL PARAMETRIC OSCILLATORS

Advantages - Wide spectral range, room-temperature operation, high conversion efficiency.

Disadvantages - Frequency-hopping; limitations on pump lasers by power thresholds, linewidth, broadening, stability in doubly resonant oscillations.

Applications - Spectroscopy, photochemistry.

Tuning Method - Rotating crystal, temperature, pressure or electric field.

Operation - Pulsed only in singly resonant oscillators, cw in doubly resonant oscillators.

of pulsed CO_2 and CO laser beams in a $CdGeAs_2$ crystal has produced beam energies greater than 75 microjoules per pulse at 16 μm.[9] A four-photon mixing experiment in alkali-metal vapor has produced tunable output between 2 and 24 μm. Mixing has the advantage of a very broad spectral tuning range, but output powers have been low and operational requirements have been very restrictive.

Gas Lasers

If one of the natural transitions of a conventional CO_2, CO, or HF laser is at the right frequency for a photochemical application, then such a laser should be used directly. While these lasers are not considered to be tunable by the usage usually accepted because the transitions are fixed within a very narrow frequency range, there are a large number of potential transition frequencies associated with each of these powerful and efficient gas lasers. It is usually desirable to utilize one of these lasers when possible.

Useful tuning ranges may be obtained with gas lasers by shifting the frequencies of the lasing transitions with magnetic fields or by operating at high pressures to broaden the gain profile.

Historically, the first tunable ir laser spectroscopy was performed by Zeeman tuning the 3.39-μm line of a He-Ne gas laser. More recently a tunability of 7 cm^{-1} was obtained with axial fields of

70 kg applied to a He-Xe gas laser operating at 3.51 μm. This technique is limited in application, as it is difficult to separate single modes and mirrors must be adjusted simultaneously with the Zeeman tuning of the atomic gas transition to avoid mode-hopping. The scarcity of high-gain laser lines and laser complexity will continue to restrict applications of Zeeman tuning.

Tunability of CO_2 laser output has been achieved by raising the pressure of the lasing gas. However, it is difficult to pump the gas and achieve lasing in high-pressure gas mixtures. Electron-beam pumping has been used with a 20-atm CO_2 laser.[10] Optical pumping has been studied for high-pressure gas lasers.

REFERENCES

1. M. J Adams and P. T. Landsberg, "Gallium Arsenide Lasers," (Interscience, New York, 1970).
2. F. Stein, "Semiconductor Lasers: Theory," in Laser Handbook (North-Holland Publishing Co., Amsterdam, 1972) p. 425.
3. H. Kressel, "Semiconductor Lasers: Devices," in Laser Handbook (North-Holland Publishing Co., Amsterdam, 1972), p. 441.
4. M. J. Colles and C. R. Pidgeon, "Tunable Lasers," Reports on Progress in Physics, 38(3) (March 1975).
5. E. D. Hinkley, K. W. Nill, and F. A. Blam, "Tunable Lasers in the Infrared," Laser Focus, 47 (April 1976).
6. R. G. Smith, "Optical Parametric Oscillators," in Laser Handbook (North-Holland Publishing Co., Amsterdam, 1972), p. 837.
7. R. G. Wenzel and G. P. Arnold, "Parametric Oscillator-HF Oscillator-Amplifier Pumped CdSe Parametric Oscillator Tunable from 14.1 μm to 16.4 μm," Appl. Opt. 15(5) (May 1976).
8. C. F. Dewey, Jr., and L. O. Hocher, "Infrared Difference-Frequency Generation using a Tunable Dye Laser," Appl. Phys. Lett. 18(58) (1971).
9. N. Barnes, R. Nickle, and P. Mace, "CO and CO_2 Mixing," Los Alamos Scientific Laboratory report LA-6353-C (June 1976), p. 83.
10. N. G. Basov et al., "Population Inversion in the Active Medium of an Electroionization CO_2 Laser at a Working-Mixture Pressure up to 20 Atmospheres," Zh. ETF Pis. Red. 17(147) (1973).

V. LASER SYSTEM RELIABILITY

Laser-system reliability is of fundamental importance in assessing the economic viability of laser-induced photochemistry and operating characteristics.

The past decade and a half of intensive laser development has witnessed the evolution of several types of experimental lasing devices into industrially rated and commercially available systems of relatively high average power. The experience gained with existing laser systems, to the extent that it applies to the tunable laser system chosen for a photochemical application, can be used as a basis for evaluating potential maintainance demands, operating requirements, and design options.

Welding Lasers

Welding lasers have been developed with heavy-duty industrial ratings and with average output power levels of the same magnitude as projected for large-scale laser photochemistry applications.

The mean life to failure has not been determined accurately, but is of the order of a year or more (10^4 h), after which the pumps and blowers require repair or replacement. Beyond these annual maintenance requirements, data are not available on projected lifetime limitations of these systems.

One large industrial laser system currently in service, a 20-kW metal-processing installation, is available more than 90% of the time.

In a continuous 20-h test of another laser system, a nominal 6-kW CO_2 open-loop, self-sustained electric-discharge laser, the power stability was maintained within ± 5% over the duration of the test (± 2% in any 15-min interval). In this test the

mode structure, measured by burn patterns in Lucite plates at 15-min intervals, remained unchanged for the duration of the test.

Manufacturers of welding laser systems indicate that the most critical components with regard to system reliability are pumps and blowers.

Pulsed High-Power CO_2 Lasers

Properly designed short-pulse high-energy CO_2 lasers normally fail in their pulser circuit. Erosion of spark gaps in the electric pulse-generating circuits is a primary mode of failure. The loss of material due to erosion requires that the spark-gap spacing be adjusted after 10^5 shots with replacement at lifetimes of $\sim 10^6$ shots.

For e-beam-pumped lasers, failures in experimental systems have frequently occurred in the pressure-vacuum window due to an arc directly hitting the window or to flying debris from an indirect arc.

Specific e-beam foil-window lifetime test data are not available. Foil windows have survived more than 10^6 shots in tests, and designs exist on paper for foils that are specified for 10^8 shots or more. Windows normally survive CO_2 laser system tests involving more than 10^5 shots at 50 pps continuous operation. The foil window in a LASL CO laser has survived more than 10^5 shots.

Nitrogen Lasers

Nitrogen lasers, being used to pump tunable dye lasers, represent a class of commercially available lasers with applications in laser photochemistry.

One manufacturer warrants its lasers for more than 10^8 pulses. These lasers utilized solid-state timing and triggering circuits incorporating a hydrogen thyratron. The duty factor for these water-cooled lasers is high.

The nitrogen lasers of slightly higher average power marketed by another manufacturer use a water-cooled two-electrode spark gap for energy switching in place of a thyratron. The switches require cleaning after $\sim 10^7$ pulses. Test spark gaps are claimed to have delivered more than 3×10^8 pulses without failure.

Dye Lasers

The lifetime of a dye-laser system is essentially determined by the mean lifetime of the pumping laser or of the flashlamps. Compared to laser-pumped dye-laser systems, flashlamp-pumped systems are much less reliable. Because the time constants associated with maintaining an inversion in dyes are short, the flashlamps are operated at high performance. Consequently, the ir lifetimes are relatively short. However, LASL has operated flashlamps for 45000 to 60000 shots without failure. Commercially available flashlamps are sealed systems. Indications are that flashlamp lifetimes could be extended by periodically replacing the gas. Flow-through flashlamp systems are being developed, but no reliability data are yet available.

Irreversible photochemical processes can occur in dye solutions, which lead to a gradual loss of laser efficiency, affecting the effective duty factor of the laser. Dye degradation is generally much more severe in broad band flashlamp-pumped dyes than for laser-pumped systems. Detailed chemical analysis of a flashlamp-pumped coumarin lasing dye indicated that optical absorption in a product of photochemical reactions accounted for the loss in laser efficiency with operating time. In systems with dye recirculation and impurity filtration and removal, the effects of dye degradation should be avoided or greatly reduced. A staged laser system in which the flashlamp pump energy is deposited in an intermediate dye (which, in turn, fluoresces at a wavelength that pumps the lasing dye with minimum breakdown) should also substantially reduce the efficiency loss due to dye degradation.

Solid-State Lasers

Solid-state (glass or YAG) lasers have off-the-shelf expected lifetimes exceeding 10^6 pulses. Lifetimes of 5×10^7 pulses are obtainable by derating the devices. The limiting components are the flashlamps for these optically pumped systems. The pumping pulse need not be as short as required for dye lasers, and the lifetime of solid-state laser flashlamps is therefore longer than that of lamps associated with dye lasers.

VI. LASER-SYSTEM SAFETY

All lasers present safety hazards peculiar to their high-voltage power supplies and their intense beams of radiant energy. The high-voltage hazards can be handled like those of any other high-voltage installation.

Containment of the laser beam and, for higher energies, remote operation are commonly used to protect operating personnel. The latter option, when required, obviously has an economic effect. Several organizations have set up standards for exposure to laser light. OSHA has adopted the American National Standards Institute standard Z136.1.

Electron-beam-pumped lasers may produce x-rays in large quantities and may require biological shielding.

Laser media may be toxic, e.g., fluorine in XeF and KrF systems. The toxicity of dyes and of dye-solvent mixtures is less obvious. Many dyes, especially cyanine and carbocyanine compounds used for generation of ir and near-ir wavelengths, are quite toxic; other dyes may be carcinogenic. At least one common solvent for these dyes, dimethylsulfoxide (DMSO), is readily absorbed through the skin and can carry any dissolved substances with it. Such materials will have to be contained and their spillage controlled in industrial environments. This is particularly important for pumped dye lasers, because flashlamps may fail violently, which would lead to dye spillage.

Failing flashlamps can ignite the highly flammable solvents used for the dyes. However, this problem can be overcome by flowmeter interlocks that shut down the power supply and the dye pumps if flow is interrupted.

The demand for safe operation of laser facilities will increase capital costs in some systems, affecting the ir scalability. Safety considerations in a large industrial laser photochemical plant could also increase operational costs, by, for example, requiring more time for maintenance than may be extrapolated from experience with small systems.

VII. PROJECTED LASER COSTS

Capital Costs

Unit capital costs, in dollars per watt (average output power), are shown as a function of average output power in Fig. 9. This curve is based on current (1976) prices for a large number of commercially available cw and pulsed, fixed-frequency, and tunable lasers. The lasers include pulsed N_2, pulsed and cw CO_2, copper vapor, cw krypton, pulsed Ar:Kr, and cw and pulsed dye lasers. They represent a wide variety of manufacturers and operating characteristics. There is relatively low scatter, considering the variety of lasers and their

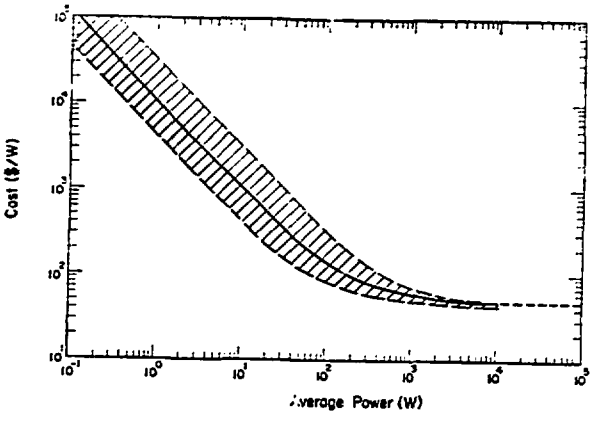

Fig. 9. Generalized relationship of purchased unit cost ($/W) to average output power (W) for commercially available pulsed and cw lasers.

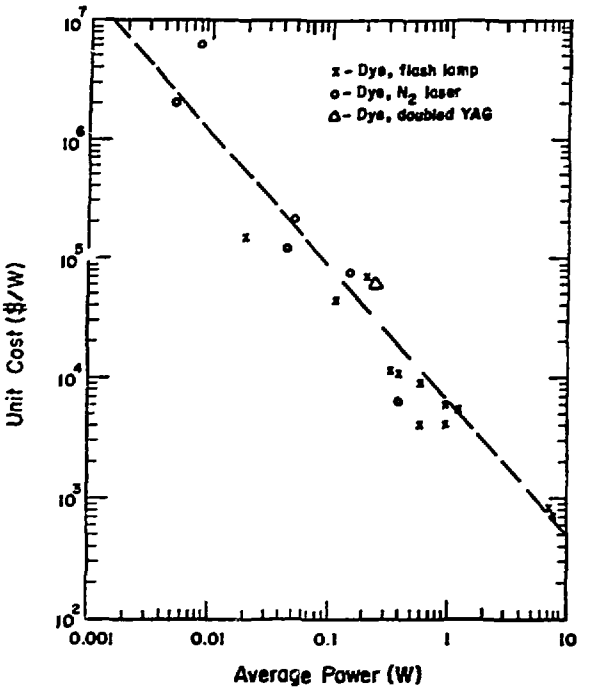

Fig. 10. Purchased unit costs ($/W) for pulsed dye lasers as a function of output power (W).

performance characteriscs. Deviations by a factor of two or more may be produced by changing the dye in a given dye laser, for example. Figure 10 indicates that this cost relationship may be extrapolated to lasers with lower average powers.

The relationship in Fig. 10 shows capital cost scaling for the major class of tunable, pulsed dye lasers. The dotted line represents the relationship given by $C = 5671\ (P)^{1.16}$ where C is unit cost ($/W) and P is average output power (W).

This scaling relationship is based on costs of 19 lasers. It may be applied over the range of average power shown in Fig. 10. The chart represents high-pulse-rate but low-pulse-energy N_2-pumped dye lasers as well as high-pulse-energy, low-pulse-rate flashlamp-pumped lasers.

Unit costs of tunable cw lasers, primarily dye and diode lasers, may be represented by a similar scaling relationship, $C = 6257\ (P)^{-0.93}$, which applies for average output power (P) in the range 0.0002 to 2.0 W.

The values of the coefficient of determination, used as a measure of quality of the fit to the power curve,[2] are 0.92 and 0.99, respectively, for the pulsed- and tunable-laser unit cost functions.

Within the precision of the data, these scaling relationships for cw and pulsed tunable lasers can be considered to be essentially identical and to extrapolate identically (Fig. 9).

The cost of a laser system is also sensitive to characteristics other than output power. Parameters that can be expected to affect costs significantly include laser efficiency, wavelength, linewidth, and beam quality.

The unit cost data do not indicate a high sensitivity to laser pulse rate. The lasers in Fig. 10 have pulse rates ranging from 1 in three seconds to 2000 per second. A good correlation of cost per joule with pulse energy in joules, Fig. 11, indicates that cost is insensitive to pulse rate for these data. In addition, the cost data also show low sensitivity to the type of laser as well as to the mode of operation.

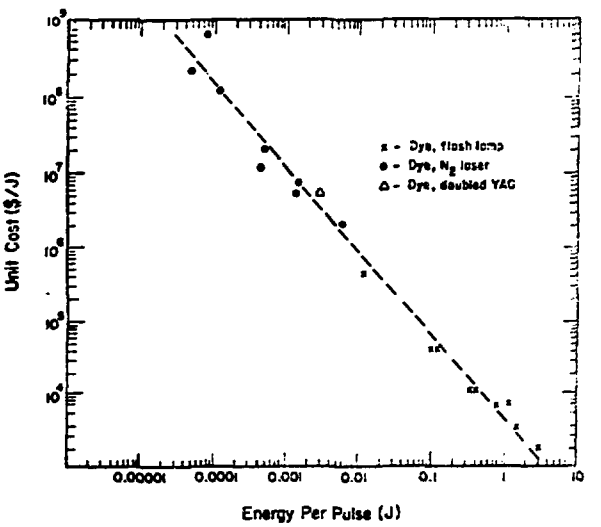

Fig. 11. Purchased costs in dollars per joule per pulse as a function of pulse energy in joules.

TABLE XIV
DYE LASER COST BREAKDOWN

Component	Cost ($)	Percent of Total
Laser tube, associated equipment	550	7.3
Power supply, flashlamps	2650	35.1
Optics, mounts, etc. (including three tuning prisms)	3050	40.4
Dye circulation and coolant equipment	1300	17.2
Total	7550	100.0

However, this insensitivity of costs to pulse rate and other laser characteristics is likely to be more apparent than real for a laser requirement with a particular combination of specifications that do not overlap with the inherent characteristics of any specific laser system.

Progress is being made in designing a specific laser to satisfy a specific photochemical reactions rather than performing the photochemistry made possible by existing lasers.

A breakdown of costs associated with functional subsystems of a dye laser is given in Table XIV. These costs are based on a recently assembled noncommercial dye-laser system, to which only $600 would have to be added for a coolant pump and refrigerator to allow sustained operation at one pulse per second. This laser has an output of ~1 J/pulse with a courmarin dye, and of ~ 2.5 J/pulse with rhodamine-6G. At one pulse per second, then, the output can vary between 1.0 and 2.5 W of average power.

The spark gaps for this laser, which require replacement, cost $350 or 4.6% of the total cost, while the capacitors cost $200 or 2.6% of the total. The dye and coolant recirculations pumps, cost $200 each or 5.3% of the total.

Operating Costs

Operating cost must include electrical power costs for the laser and for auxiliary equipment, the costs of replacement parts, and the costs of special materials such as cryogenic coolants and makeup dye.

Electrical power costs are important where the net efficiency of the laser is low or in those photochemical applications where excess laser power is required because the absorption or reaction cross section is low. A simple relationship for annual cost of electricity may be of the form

$$C_e = 0.175\ fd(P/\eta + Paux),$$

where

C_e = annual cost of electricity,
fd = annual duty factor,
P = laser average output power (W),
Paux = power required by auxiliary equipment (W), and
η = laser efficiency.

The unit cost of electricity is assumed to be 20 mills/kWh.

The cost of replacement components depends on the system, its inherent reliability, and on the relationship between operating parameters and rated performance. Generally, if the components of a laser system are operated well below their rated performance level, mean life to failure will be substantially enhanced. In the absence of reliable data from a specific system, annual replacement costs have been estimated at 25% of the original cost.

The costs of special materials will depend entirely on the nature of a specific laser system and its operating conditions. With dye lasers, makeup dye must be purchased to replace losses due to dye degradation. Depending on, e.g., the type of dye, solvent, and optical pumping source used, this cost could vary from a trivial expense to a very substantial one. With recirculation and filtering, the dye replacement expense should not be excessive. Unfortunately, the design of most dye lasers does not provide adequate quantative information about dye replacement. With gas lasers,

including rare-gas excimers, the gas may be regenerated and recirculated, otherwise replacement gas costs could be prohibitive in many applications.

REFERENCES

1. "1976 Buyers' Guide," Laser Focus (February 1976).
2. K. A. Brownlee, Statistical Theory and Methodology in Science and Engineering (John Wiley and Sons, 1965).

ACKNOWLEDGMENTS

This study was funded by Brookhaven National Laboratory as a portion of the "Assessment and Analysis of Separation Schemes Applied to Reactor Waste Management," a study conducted by M. Goldstein of Brookhaven National Laboratory. This study was conducted during fiscal year 1976 by C. K. Rofer-DePoorter, F. T. Finch, and H. C. Volkin of the Los Alamos Scientific Laboratory (LASL) Laser Division. Assistance was received from many Laser Division Staff Members, especially L. A. Booth and G. L. DePoorter.